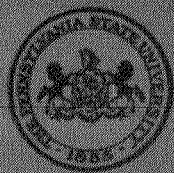


N70 32493



THE PENNSYLVANIA
STATE UNIVERSITY

NASA CR 110646

IONOSPHERIC RESEARCH

Scientific Report No. 356

DOUBLE LANGMUIR PROBE MEASUREMENTS IN A MAGNETIZED POSITIVE COLUMN

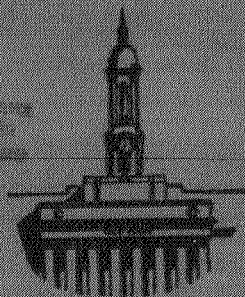
by

V. C. Dunham

May 15, 1970

IONOSPHERE RESEARCH LABORATORY

CASE FILE
COPY



University Park, Pennsylvania

NASA Grant NGL 39-009-003

Ionospheric Research

NASA Grant NGL 39- 009-003

Scientific Report

on

"Double Langmuir Probe Measurements in a
Magnetized Positive Column"

by

V. C. Dunham

May 15, 1970

Scientific Report No. 356

Submitted by: J. S. Nisbet (aw)
John S. Nisbet, Professor of Electrical Engineering
Project Supervisor

Approved by: A. H. Waynick
A. H. Waynick, Director
Ionosphere Research Laboratory

Ionosphere Research Laboratory
The Pennsylvania State University
University Park, Pennsylvania

16802

ABSTRACT

A study is presented of the positive column of a cold cathode, cylindrical glow discharge in nitrogen (.2 and 1.0 Torr) under the influence of a small, approximately uniform, longitudinal magnetic field (0-200 gauss). To supply a background for the study, a survey is made of the theories of glow discharges and both single and double probes with and without magnetic fields.

Using double cylindrical probes, measurements were made in the positive column to determine the effect of the magnetic field on the electron temperature and density. For $B=0$, the temperature and density are shown to agree with the theory, the former being constant across the column, and the profile of the latter being described by the zero order Bessel function.

For $B \neq 0$, the temperature decreases more rapidly than the theory predicts for increasing B , but becomes constant for $B = 100-200$ gauss. The axial density is shown to increase nearly at the rate predicted by the theory.

No conclusions are made concerning the effect of non-uniformity of the field on the double probe method since the exact behavior of the positive column is not known for the type of field used.

TABLE OF CONTENTS

Abstract	i
I. THEORETICAL	1
A. Introduction	1
B. Definition of Symbols	3
C. Theoretical Background	4
1. The Glow Discharge	4
a. General Description	4
b. The Positive Column, $B=0$	7
c. The Positive Column, $B \neq 0$	13
2. Single Langmuir Probes, $B=0$	16
a. The Dilute Case	16
b. The Continuum Case	20
c. The Intermediate Case	21
3. Single Probes, $B \neq 0$	22
4. The Double Probe Method, $B=0$	24
a. Determination of Electron Temperatures	29
b. Determination of Plasma Density	33
5. Double Probes, $B \neq 0$	35
II. EXPERIMENTAL APPARATUS AND PROCEDURES	39
A. Apparatus	39
1. Supporting Equipment	39
2. The Probes	46
B. Procedures	49
III. RESULTS AND DISCUSSION	54
A. The Positive Column, $B=0$	54
B. The Positive Column, $B \neq 0$	59
IV. SUMMARY	66
BIBLIOGRAPHY	69
APPENDIX	72

LIST OF FIGURES

Figure		Page
1	A Typical Glow Discharge	5
2	CPR vs. Electron Temperature/Ionization Potential (von Engel and Steenbeck)	11
3	Helium Positive Column Electron Temperature vs. RP.	11
4	Double Probe Circuit.	25
5	Double Probe Characteristic Curve (Current vs. Voltage).	27
6	Experimental Apparatus.	40
7	Discharge Tube, Magnet and Co-ordinate System . .	42
8	Magnetic Field on the z-axis.	43
9	Gradient of B_z vs. Radial Position and Magnetic Field	44
10	Description of the Probes	47
11	Typical Current vs. Voltage Curves for Air and N_2 (Probe Set Number One)	55
12	Electron Temperature vs. Radius	56
13	Relative Density vs. Radius	57
14	Relative Electron Temperature and Density vs. Magnetic Field.	62
15	Saturation Ion Currents vs. Magnetic Field. . . .	64
16	Sample Calculation Curves	73

I. THEORETICAL

A. Introduction

One of the first techniques for measuring the properties of plasmas was developed by Langmuir and his co-workers, (1926). The technique is sometimes referred to as the single probe method (SPM). The probe itself is simply an electrode inserted in a plasma and biased relative to any other electrode in good contact with the plasma. The important thing to note is that the probe is actually being biased relative to space potential. The current collected by the probe when used in this fashion indicates the magnitudes of plasma parameters such as electron temperature and density, and space potential.

The SPM is widely used today in a variety of plasmas; however, there are some limitations which sometimes make its use undesirable. One such limitation is the fact that under certain conditions the current drawn by the probe is of sufficient magnitude to perturb the plasma appreciably. When this is the case, the SPM is not the best method to measure the plasma parameters.

One example of such conditions is that of a low density glow discharge. The current density in such a discharge is low enough that the probe current is comparable in magnitude. In most cases when this is true, the perturbations of the glow column are clearly visible. The obvious conclusion is that the SPM should not be used when perturbations of this magnitude result.

A method developed by Johnson and Malter (1950) to study time varying plasmas avoids this problem. In this, the double probe method (DPM), the probes collect only a small current and thus disturb the plasma to a minimum degree.

This method has been used for some time to investigate conditions in a variety of plasmas. It too has limitations, but the advantages for the type of study described in this report are apparent. One of the limitations which will be discussed later is the very small fraction of the electron population sampled by the probes as they float with space potential. The most striking advantage is that the probes do not disturb the plasma to any important degree.

Often the conditions surrounding the experimental production or examination of plasmas involve magnetic fields, either for confinement or for other reasons. For example the study of trapped plasmas in various types of magnetic enclosures is common. Magnetic mirrors and bottles with non-uniform fields are used widely for confinement of various plasmas. The DPM to be useful enough to warrant attention should then be effective in these types of experiments where magnetic fields are present.

The reliability of the DPM in a magnetic field has been studied by Sugawara and Hatta (1965B). They showed that for low or moderate fields the method indicated conditions which agreed with theoretical studies, in this case, the glow discharge.

The present study considers the positive column of a cylindrical glow discharge in a longitudinal magnetic field. A comparison is made between the theoretical description of the column and the experimentally determined description. The comparison is made through the effects of the magnetic field on the plasma parameters, i.e., the electron temperature and density.

In this study the discharge was operated at two pressures, .2 and 1.0 Torr, and in two gases, pure nitrogen and air. All measurements made by probes were made by cylindrical double probes used in the fashion of those described in the work of Johnson and Malter.

The first section of the report surveys the theoretical work on probes that has a direct bearing on the study of plasmas by electrostatic probes. Single probes are included due to their similarity and historical importance in the development of the theory of the double probe. It is noted, however, that the DPM is the more general method.

The experimental apparatus and the procedures followed to collect the data are described in detail in the second section, followed by a discussion of the results in section three.

B. Definition of Symbols

A_a = probe area

A_s = sheath area

a = probe radius

B = magnetic induction (gauss)

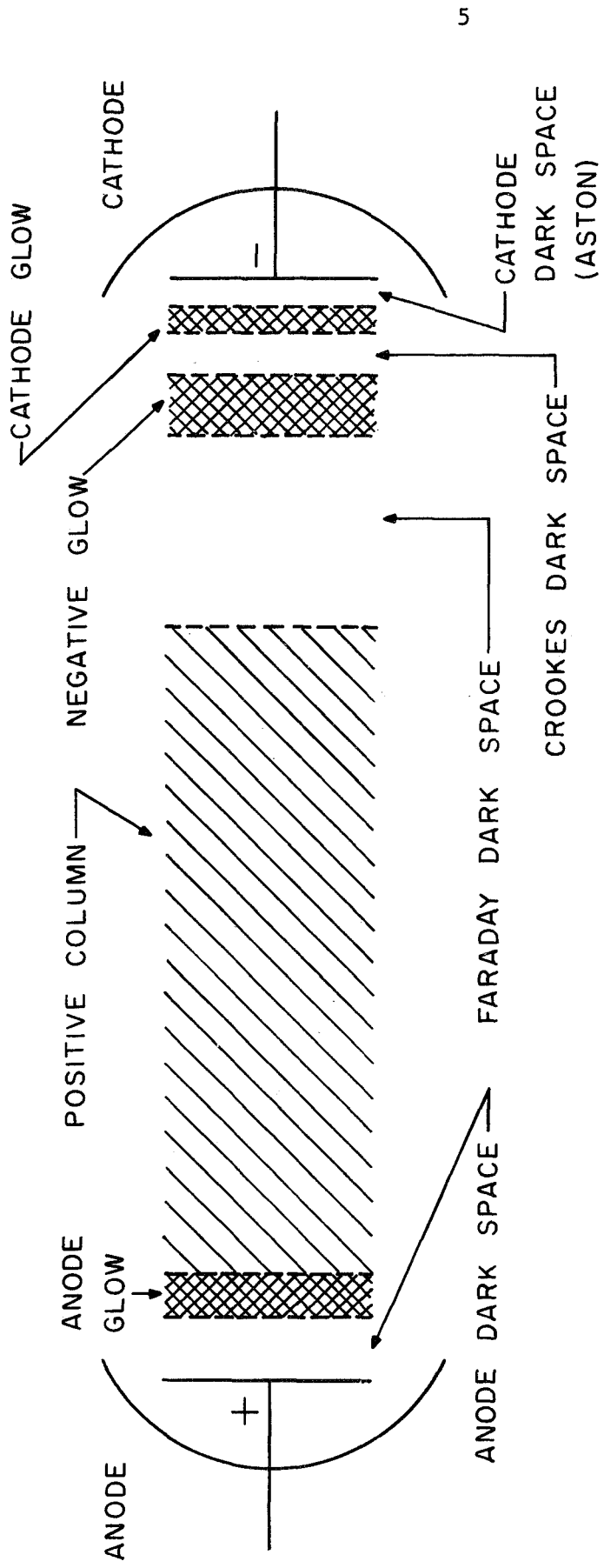
C = capacitance
 D = diffusion coefficient
 D_a = ambipolar diffusion coefficient
 I = current
 k = Boltzmann's constant
 l_D = Debye length
 l_- = mean free path for electrons
 l_+ = mean free path for positive ions
 m = mass
 n_- = number density of electrons
 n_+ = number density of positive ions
 P = neutral gas pressure
 ρ_- = Larmor radius for the electron
 ρ_+ = Larmor radius for the positive ion
 R = radius of the discharge tube
 T_- = electron temperature
 T_+ = positive ion temperature
 V = potential or voltage

C. Theoretical Background

1. The Glow Discharge

a. General Description

The glow discharge is one of the many types of discharges in gases. Its characteristics are the subject of a prodigious amount of literature of which two books by Sanborn C. Brown (1959 and 1966) are an excellent review. Figure 1 is a representation of a typical glow discharge.



A TYPICAL GLOW DISCHARGE

FIGURE 1

The glow discharge is maintained by electrons produced at the cathode by positive ion bombardment. The appearance of the discharge may be complicated as indicated by the figure. Beginning the description at the cathode, the cathode glow is caused by the decay of positive ions from excited states upon neutralization by electrons. As the electrons are accelerated by the electric field of the Crookes dark space, they gain enough energy to cause inelastic collisions. The excitation of the gas gives rise to the negative glow.

The range of the most energetic electrons which produce this excitation is indicated by the positive end of the negative glow. As the electrons are again accelerated, there is a region of relative darkness called the Faraday dark space just before the positive column.

The positive column extends from the Faraday dark space to the glow near the anode. The column is not essential for the maintenance of the discharge and in short tubes may be absent altogether. Since there is little or no net space charge in the positive column it is essentially a neutral or quasi-neutral plasma which lends itself readily to study by electrostatic probe techniques. It is this region in which all of the probe measurements were made. In the last few mean free paths before the anode, electrons gain sufficient energy to cause excitation and the anode glow results.

b. The Positive Column, $B=0$

Considering now the positive column in more detail, the quantities of interest are the radial distribution of charge, the electron temperature, and the radial and longitudinal electric fields. These quantities were expressed by von Engel (1965) with the limitation that $P=1-10$ Torr, $R=1-10$ cm., and $I=10^{-4}-1$ amp. (where I is the discharge current). Our experimental parameters are within these limitations.

The radial distribution of charge is primarily governed by the rate of ionization and recombination and by the rate of loss due to diffusion to the walls. The longitudinal electric field must be high enough so that the number of electrons and ions produced per second just balances the loss of charge by diffusion and recombination.

Schottky (1924, 1925), assuming that the mean free path for electron-neutral collisions is much smaller than the tube radius, i.e., the electrons make many collisions in drifting a distance R , and assuming that ionization is produced by single collisions only, developed the theory of ambipolar diffusion by which both ions and electrons drift away from the axis with equal velocities.

The phenomenon of ambipolar diffusion is explained in the following manner. Due to their lighter mass the electrons tend to diffuse out of the plasma at a faster rate than the positive ions. The charge separation that results sets up an electric field which retards the free diffusion of the electrons and

simultaneously enhances the diffusion of the positive ions. The result is that the positive ions and electrons diffuse together at an intermediate rate.

Ambipolar diffusion is present in discharge plasmas when the electron density exceeds, approximately $10^8/\text{cm}^3$, then the electric field produced upon charge separation retards the free diffusion of the electrons.

At any rate, assuming $l \ll R$ and $n_- \approx n_+ = n$ and $d\mu_+/dr \approx dn_-/dr = dn/dr$, by matching the rate of ionization with the diffusion losses, von Engel (1965) derives a differential equation which gives the radial distribution of charge.

$$\frac{d^2 n}{dr^2} + \frac{1}{r} \frac{dn}{dr} + \frac{z}{D_a} n = 0. \quad (1)$$

where z = the number of ionizations produced per electron per second and D_a = the ambipolar diffusion coefficient defined as follows.

$$D_a = \frac{\mu_+ D_- - \mu_- D_+}{\mu_+ - \mu_-} = \frac{D_+ D_- (T_+ + T_-)}{D_- T_+ + D_+ T_-} \quad (2)$$

where μ = the mobility of either the electron or ion and where the expression $D_-/\mu_- = kT_-^{-1}$ (Einstein relation) has been used. Since $T_- \gg T_+$ in the present case,

$$D_a \approx \left(1 + \frac{T_-}{T_+}\right) D_+ \approx D_+ \frac{T_-}{T_+} \quad (3)$$

The solution to equation (1) is

$$n_r = n_o J_o (r\sqrt{z/D_a}) \quad (4)$$

where n_o is the density at $r = 0$ and J_o is the first-order Bessel function. The boundary condition on this solution is the following.

$$n_r/n_o \Big|_{r=R} = 0 \quad (5)$$

Therefore, $R\sqrt{z/D_a} = 2.405$, the first zero of the Bessel function J_o . Hence,

$$n_r = n_o J_o \left(\frac{2.405 r}{R} \right) \quad \text{and} \quad \sqrt{z/D_a} = \frac{2.405}{R} \quad (6), (7)$$

The boundary condition arises from the fact that the ions and electrons recombine on the walls and hence the density of charged particles must approach zero as $r \rightarrow R$.

To find an expression for the electron temperature equation (7) is useful. As developed by von Engel and Steenbeck (1932) the ionizing frequency z can be written

$$z = \frac{600 a}{e\sqrt{\pi}} m \rho \alpha^3 \left(\frac{1}{2} \frac{eVi}{kT_-} \right) \exp \left(-\frac{eVi}{kT_-} \right) \quad (8)$$

where "a" is a measure of the efficiency of ionization, α is the probable thermal velocity $(2kT_-/m)^{1/2}$. Let $\eta = eVi/kT_-$ and use equation (7) and the electron temperature is related to R.

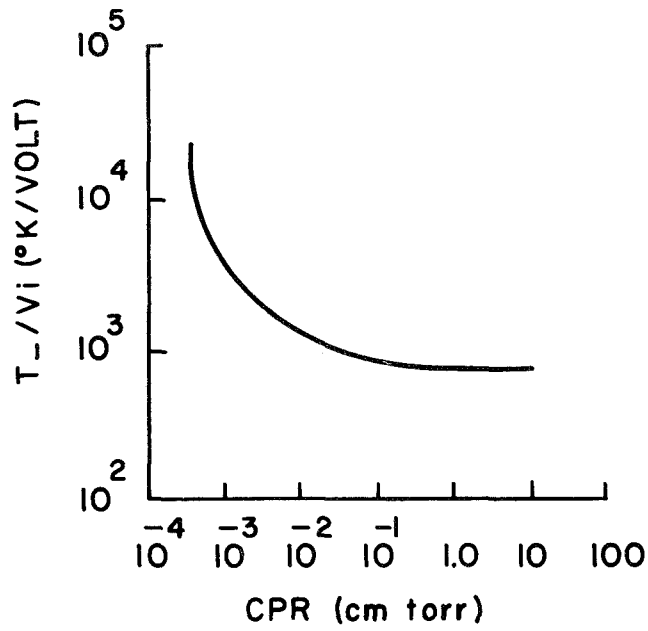
$$\frac{1}{\eta^{1/2}} \exp(-\eta) = \frac{600\sqrt{2e}}{(2.405)^2\sqrt{\pi m}} \frac{a\sqrt{v_i}}{\mu P} P^2 R^2 = 1.16 \times 10^7 c^2 P^2 R^2 \quad (9)$$

where $R(\text{cm})$, $P(\text{Torr})$, $V_i(\text{volts})$, $\mu_+(\text{cm}^2/\text{volt-sec})$ and $c^2 = aV_i^{1/2}/\mu_+P$. Von Engel and Steenbeck (1932) have plotted a curve T_-/V_i vs. cPR and have calculated c for different gases. For nitrogen $c = 3.5 \times 10^{-2}$. Therefore using the curve of Figure 2 and the value of cPR , the electron temperature of the positive column can be estimated.

Bickerton and von Engel (1956) found for helium that rather than the electron temperature predicted by the Schottky theory, their experimental results more closely fit the curve of the theory of Tonks and Langmuir (1929) which is a long l_+ theory. This is illustrated in Figure 3.

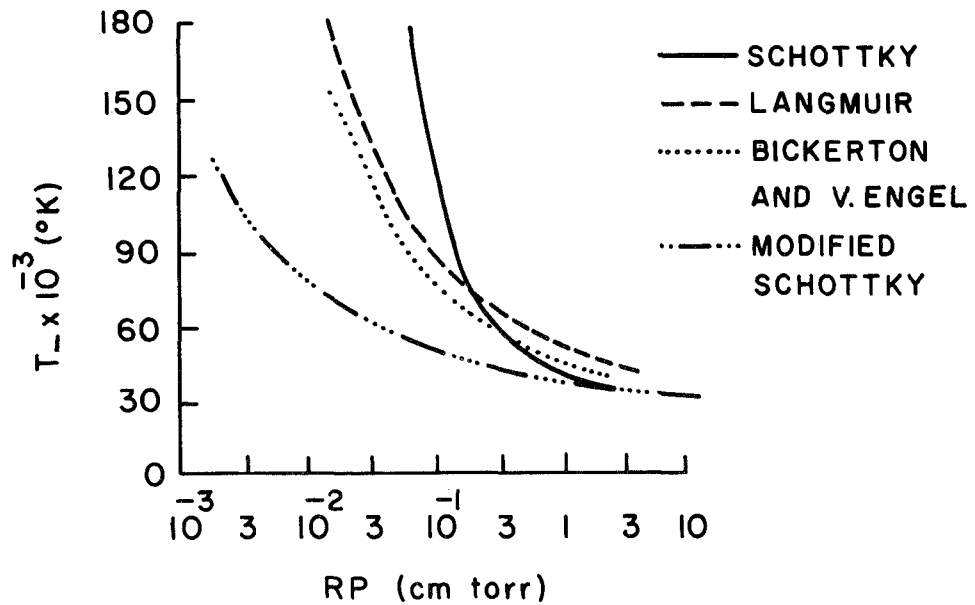
The curve labeled Langmuir is derived from the work of Tonks and Langmuir. Therefore, it can be seen that Bickerton and von Engel found that for helium, the positive column was described by an electron temperature indicative of a column where the mean free path for ions was large relative to the tube radius, even though the pressure range used indicated mean free paths shorter than the tube radius. They suggested that this was due to a large radial electric field resulting from the high electron temperature found in the rare gases.

Bickerton and von Engel also developed what they called the modified Schottky theory for the dependence of the electron



CPR VS ELECTRON TEMPERATURE/IONIZATION POTENTIAL (VON ENGEL AND STEENBECK)

FIGURE 2



HELIUM POSITIVE COLUMN ELECTRON TEMPERATURE VS RP

FIGURE 3

temperature on RP. The radial distribution of charge found by Schottky remains valid, i.e.,

$$n_r = n_o J_o(\sqrt{z/D_a} r) \quad (4)$$

Continuing with their derivation, let $x = (z/D_a)^{1/2} R$. Then the flow density of ions to the walls is

$$\frac{j}{e} = \frac{\bar{n}_w v_+}{4} = \frac{\bar{n}_o v_+}{4} J_o(X) \quad (10)$$

By bringing in the relationship of z to T_- their result was

$$\frac{4}{R} \frac{D_a}{v_+} = \frac{1}{X} \frac{J_o(X)}{J_1(X)} \rightarrow \frac{4}{3} \frac{l_+}{R\rho} \frac{T_-}{T_+} = \frac{1}{X} \frac{J_o(X)}{J_1(X)} \quad (11,12)$$

where $D_a = 1/3(1_+ v_+ T_-/T_+)$ and $1_+\rho = 1_+$ and where J_o and J_1 are Bessel functions of order zero and one respectively. The experimental data they collected all falls between the curve labeled Schottky and the modified Schottky theory in Figure 3. The most striking development of the modified Schottky theory is the dependence of D_a on z which is no longer a simple linear function.

Bickerton and von Engel developed this theory to circumvent the assumption that the density of charged particles near the walls of the tube was much smaller than the density on the axis. The assumption was shown invalid even for small l_+ by considering the equality between the number of ions lost per unit length and the number produced per unit length in the column.

In summary, the quantities of interest in the positive column are the radial distribution of charge, the electron temperature, and the electric fields. The radial distribution of charge is given by equation (4) derived from the Schottky theory of ambipolar diffusion. There seems to be general agreement as to the validity of this expression.

Several determinations of the electron temperature were mentioned beginning with that of von Engel and Steenbeck (1932) given in Figure 3. Bickerton and von Engel (1956) found that the theory of Tonks and Langmuir (1929) more closely predicted the electron temperature of a helium positive column than the theory of Schottky (1924, 1925).

c. The Positive Column, $B \neq 0$

The particles in the positive column of a glow discharge have velocity components in all directions, having essentially a Maxwellian velocity distribution function. When a magnetic field is applied in the anode-cathode (longitudinal) direction, the motion of the electrons and ions is somewhat altered in a direction perpendicular to the field. The particles move in helical paths spiraling around the magnetic field lines of force.

This picture must be altered when the mean free path for collisions is comparable to or less than the Larmor radius. The electrons having the smaller mass, are affected most by the field

which reduces their diffusion to the walls of the tube. Since the number of ions arriving at the wall must be equal to the number of electrons there, the reduction of radial motion by the magnetic field on the electrons also produces a reduction of ionic radial motion. The mechanism by which the ionic motion is reduced is the radial electric field. The reduced radial motion of the electrons produces a reduction in the electric field which in turn reduces the radial motion of the ions.

The reduction in loss of charge due to the diffusion reduction also has an effect on the electron temperature which is diminished also. Bickerton and von Engel (1955) use the equation

$$\frac{4}{3} \frac{I_+}{RP} \frac{T_-}{T_+} = \frac{1}{x} \frac{J_0(x)}{J_1(x)} \quad (13)$$

to calculate the change in T_- due to the magnetic field. This change is introduced through the value of T_+ which changes due to the change in the radial electric field.

The reduction in diffusion as a function of magnetic field is seen in the diffusion coefficients.

$$D_{\perp-} = \frac{D_-}{1 + (\tau_- \omega_-)^2} \quad (14)$$

where $D_{\perp-}$ is the electron diffusion coefficient perpendicular to B and D_- is the electron coefficient for $B = 0$. τ_- is the electron-neutral collision time and ω_- is the electron cyclotron frequency.

$$D_{\perp a} = \frac{D_a}{1 + (\omega_- \tau_- \omega_+ \tau_+)} \quad (15)$$

is the ambipolar diffusion coefficient in a magnetic field, with τ_+ being the positive ion-neutral collision time and ω_+ being the ion cyclotron angular frequency, (Holt and Haskell, 1965).

Bickerton and von Engel found that for their experiments "The reduction in electron temperature through the influence of the magnetic field on the ambipolar diffusion coefficient is here of an altogether smaller order than that due to the influence of B on the radial electric field (transition from Langmuir to modified Schottky theory)."

The conclusions of Bickerton and von Engel are that when the magnetic field is applied to the positive column, (1) the motion of the electron and ions radially approaches the modified Schottky theory, i.e., small radial drift with respect to mean velocities, (2) the radial distribution of charge is altered and the density on the axis rises, (3) when the current is low and constant, the increase in the number of electron/length along the axis reduces the longitudinal electric field, (4) the effect on the electron temperature comes about mainly from the reduction of the radial electric field rather than from the reduction in diffusion through the ambipolar diffusion coefficient.

2. Single Langmuir Probes, $B=0$

a. The Dilute Case

The SPM has been used widely to study plasmas. It is a simple experimental approach to diagnostics and gives local readings as opposed to microwave or spectroscopic methods which may not. First consider the theory's basic characteristics.

Sanmartin (1968) divides the theory of single probe into three basic categories according to the nature of the plasma the probe is in. This division is made relative to the important plasma parameters in the problem. Three lengths are a natural dividing mechanism. They are l_D , the Debye length, a measure of the range of the potential gradients around an electrode; "a", the probe radius; and l , the mean free path. Using these symbols, the categories are: (1) $l_D \ll a \ll l$, the dilute case where the mean free path is the largest parameter, (2) $l \ll l_D \ll a$, the continuum case where the plasma is collision dominated, and (3) $l_D \ll l \ll a$, the intermediate case.

These three cases will be discussed briefly including a simple mathematical description of each. The discussion will be limited mainly to cylindrical probes and the collection of positive ions. The reason for these limitations is that in the double probe theory the saturation ion current is the quantity from which the plasma parameters are derived. Since the probes are saturated one at a time, the method is similar to the single probe case in this respect. First consider the dilute case.

Many authors have developed the theory for this case of whom Bernstein and Rabinowitz (1959), Lam (1965), and Bienkowski (1967) are the most recent contributors. Chen (1965) gives an excellent survey of the electrostatic probe in the dilute plasma as well as the continuum case. Assuming the conditions of the dilute case, Allen et.al., (1957) showed that for a spherical probe collecting ions of one energy and traveling in a radial direction only, the saturation current is

$$I = .61 A_{\rho} \left(\frac{kT_{-}}{m_{+}} \right)^{1/2} n_0 \quad (16)$$

Here the sheath radius was assumed at $\eta_{\rho} \approx 1/2$ and $\xi_{\rho} \approx a/l_D$ at the sheath where $\eta_{\rho} = -eV/kT_{-}$ and $\xi_{\rho} = r/l$. Equation 16 was derived for the zero temperature case where the ions start from rest at infinity ($V=0$) and move radially toward the spherical probe. The total current to the probe is $I=4\pi r^2 n_{+} v_{+}$ where $v_{+} = (-2eV/m_{+})^{1/2}$ and V is the potential. It can be seen that $v_{+} = v_s \eta^{1/2}$ where $v_s = (2kT_{-}/m_{+})^{1/2}$. Since in the absence of collisions and ionization I is conserved, using $n(I)$ in Poisson's equation with the usual change to dimensionless variables, the approximate solution, Equation 16 is obtained. (See Chen, 1965, p. 139.) This discussion was included (although the probes used in our study were cylindrical) since the insensitivity of the constant factor to the ion temperature as shown by Bohm (1949) gives an indication why the theory does not give the ion temperature by direct measurement.

Perhaps one of the most straight-forward methods for determining the plasma density once the saturation current is found is the theory of Lam (1965). This treatment includes the following expressions.

$$\frac{-V_{\rho}}{(eI_{+a})^{2/3}} = \left(\frac{2m_{+}}{e}\right)^{1/3} \Lambda_c(\tau) \quad (17)$$

where $\tau = I_{+}/I_B$ and $I_B = 1.9 a n_o v_s$ and $v_s = (2kT_{-}/m_{+})^{1/2}$. A constant $A = 2.2$ (for cylinders) also enters the theory and includes the dependence of the saturation current on the potential. Λ_c is a function calculated by Lam, and $\tau = I_{+}/I_B$ as before. The plasma density is found in the following manner. The L.H.S. of equation (17) is computed using the measured I_{+} , the saturation ion current. Hence we know the value of Λ_c . By use of Figure 14 of Huddleston and Leonard (p. 150) the value of τ can be found. Therefore we know the value of I_B and hence the density n_o .

The ion saturation currents for the dilute case mentioned do not consider the end effects near a finite cylinder. Electron collection for low potentials is also neglected. In most cases where the much colder species is collected, the original theory of Langmuir and Mott-Smith (1926) does not apply since an absorption radius, much larger than the radius of the probe, usually exists.

At any rate, Bohm, Burhop, and Massey (1949) derive an expression which is a rough approximation to the ion saturation current to any shaped probe even in a magnetic field. The appropriate area must be inserted however.

$$I = 1/2 n_o A \rho \left(\frac{kT_-}{m_+} \right)^{1/2} \quad (18)$$

No dependence on the probe voltage is given since the sheath edge approximation was made. Although this is perhaps only an order of magnitude estimate of the current, it is very useful when A is known in a magnetic field. The dependence on n and T is explicit.

The theory of Lam gives the dependence of I on the potential for large ξ_ρ and η_ρ . It is perhaps the most straight-forward method of determining the plasma density. Since the probes used in the present experiment are cylindrical, the work of Chen (1965B) which supplements the theory of Lam for spherical probes, could be used as well.

When $l_D \gg a$ the equations governing the motion of the plasma must be solved numerically. Bernstein and Rabinowitz (1959) provide a method similar to that of Lam for the calculation of n_o . This was done for spherical probes and extended to cylindrical probes by Chen.

All of the theories mentioned, suffer from the fact that the electric field of the probe accelerates ions from large distances and hence collisions and external electric fields are apt to affect the probe current.

b. The Continuum Case

Collisions must be considered in the continuum case where either $l_D \gg 1$ or $l \ll a$. Let the following dimensionless variables be introduced.

$$\eta = \frac{-eV}{kT_-}, \quad \rho = r/l_D, \quad i = I/I_0, \quad I_0 = \frac{2\pi n_0 \mu_+ kT_-}{e_+} \quad (19)$$

where $l_D^2 = kT_- / 4\pi n_0 e_+^2$ and $\mu_+ = l_+ D_+ / kT_+$ and D_+ is the diffusion coefficient for classical diffusion. Chen derives the following expression for the saturation current.

$$\eta - \eta_s = i^{1/2} \left\{ \left(\sigma^2 - \rho^2 \right)^{1/2} - \sigma \log \left[\frac{\sigma}{\rho} \left(\frac{\sigma^2}{\rho^2} - 1 \right)^{1/2} \right] \right\} \quad (20)$$

where $\sigma/P = s/a$, where $\sigma = s/l_D$ and $\rho = a/l_D$ and s = the sheath radius. By substituting the variables in equation (20), the current I is shown to be dependent on $(V - V_s)^2$ rather than on $(V - V_s)^{3/2}$ as in the collisionless case. Chen provides derivations of current to spherical probes and to cylindrical probes at space potential, but these will not be discussed here.

Most recent studies of the continuum case were made by Su and Lam (1965) and Cohen (1963). The work of Chen just mentioned is more easily applied and will be considered adequate to cover the basic differences between the dilute and continuum cases. In general it can be said that when the mean free path is neither small nor large, the theory becomes extremely complicated since there is no simple equation of motion. This case was first

considered by Davydov and Zmangvskaja (1936) with $l_D=1$. They included ionization, but seemed to be unfamiliar with the sheath criterion. Boyd (1951) treated the problem by dividing the space near the probe into four regions and then matching boundary conditions. The result was that the probe current could not be computed without prior knowledge of the sheath radius.

c. The Intermediate Case

The transition from the collisionless to the collision-dominated case was given by Schulz and Brown (1955). They used equation (20) for the collision dominated case obtained excellent agreement with microwave measurements.

Ecker et. al., (1962) showed that the primary effect of collisions was to decrease the plasma density at $r=1$ due to the blocking effect of the probe. The magnitude of the decrease is given by

$$n_\lambda/n_o = \frac{4\pi CD}{4\pi CD + \bar{v}A_p/4K} \quad (21)$$

where C is the capacitance of the probe, \bar{v} is the magnitude of the thermal velocity, and K is a constant between 1 and 1/2 depending on the relative sizes of the radii of the probe and sheath.

Su and Lam also developed theories for this case for spherical probes, as did Cohen, but equation (20) can be used if the sheath thickness can be estimated. The most recent work

done on this case was by Chou, Talbot, and Willis (1966), Boyd (1951) and Su (1968).

Since the plasma of a positive column has a certain drift velocity, its effect if any on the probe current should be calculated. If the estimate of the longitudinal electric field given by Brown (1959) is used, and the following expression for the drift velocity is valid,

$$v_D^{\max} = \frac{F\Delta t}{m_+} = \frac{1 + E_0 \tau_+}{m_+} \quad (22)$$

where τ_+ = the mean free time, then the drift current is found to be 4.0×10^4 cm./second. With the positive ion temperature of 3.5×10^2 K, the ratio $v_+^{\max}/v_+ = 1.2$. Hence, according to the theory of Langmuir (1961, p.116) the electron temperature can be expected to be measured no more than five percent in excess of the true value. Since this is within the experimental error, the effect of the drift cannot be distinguished. Therefore we assume that the drift is not important in the calculation on the electron temperature and density. Strictly speaking the Langmuir theory does not exactly apply in this case, but the effects of collisions in the sheath which it neglects do not, it seems, make a great difference in approximating the ion saturation current.

3. Single Probes $B \neq 0$

Chen (1965A) gives an excellent discussion of the over all problem of the probe in a magnetic field and this discussion will

be briefly reviewed. First of all, the magnetic field decreases the saturation electron current below its value in a zero field. The field also tends to destroy electron saturation. It is likely however that the slope of the transition region still gives the electron temperature at least for moderate fields. By moderate fields we mean that the magnetic field is weak enough so that electrons are in equilibrium. For high fields where there is not equilibrium the slope most likely would give an indication of the temperature of electrons in motion parallel to the magnetic field since they are nearly the only ones collected.

Another effect is that the intersection of the slope of the transition region and the slope of the electron saturation region no longer is an indication of the space potential. Finally, the ion saturation current for weak fields should not be greatly affected, but when the Larmor radius (ions) is smaller than or nearly equal to the other relevant dimensions in the plasma and probes, to date no successful attempts to indicate the current have been made.

The theory of Bohm [Burhop and Massey, 1949], as mentioned in the discussion of the zero field case, includes an equation which approximately gives the ion saturation current.

$$I = 1/2 n_0 A \left(\frac{kT_-}{m_+} \right)^{1/2} \quad (23)$$

This relation holds for moderate fields where $\rho_- \ll a \ll \rho_+$ where ρ is the Larmor radius for either electrons or ions according to the second subscript. The value for A may or may not be the probe area depending on the configuration and orientation in the magnetic field.

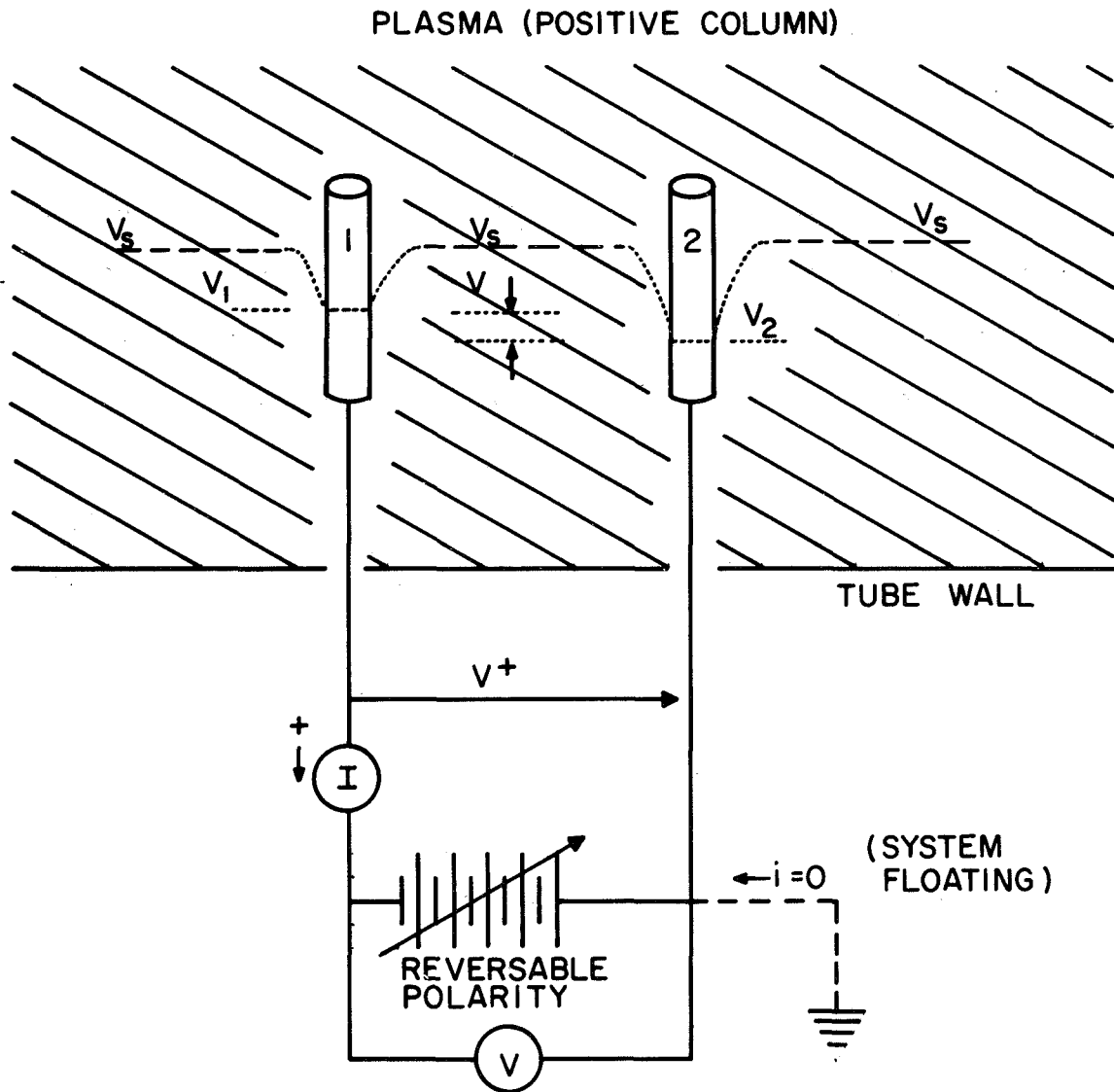
Sanmartin (1968) points out that the work of Bertotti (1962), as mentioned and enumerated in Chen, is in contradiction with experiment since the current in the magnetic field is larger than for the zero field case. Sanmartin also mentions the fact that the work of Spivak and Reichrudel (1938) and Bickerton and von Engel (1956) each introduce an ill-defined sheath edge where the density cannot be expected to be that of the unperturbed plasma.

For saturation ion current, no satisfactory theory exists. However if the electrons are in thermal equilibrium and the ion Larmor radius is much larger than the probe dimension, the normal theories for ion collection may be used (see Single Probes, $B=0$).

4. The Double Probe Method, $B=0$

The Double Probe Method (DPM) developed by Johnson and Malter (1950) is a diagnostic technique for use in unstable plasmas. The method has been successfully applied to quiescent plasmas and lends itself directly to the study of the glow discharge. In the case at hand the method was used to investigate the plasma conditions of the positive column of a glow discharge.

The DPM employs the use of two probes not at all unlike single Langmuir probes. They are connected to a variable voltage source as shown in Figure 4. By the application of a voltage



DOUBLE PROBE CIRCUIT

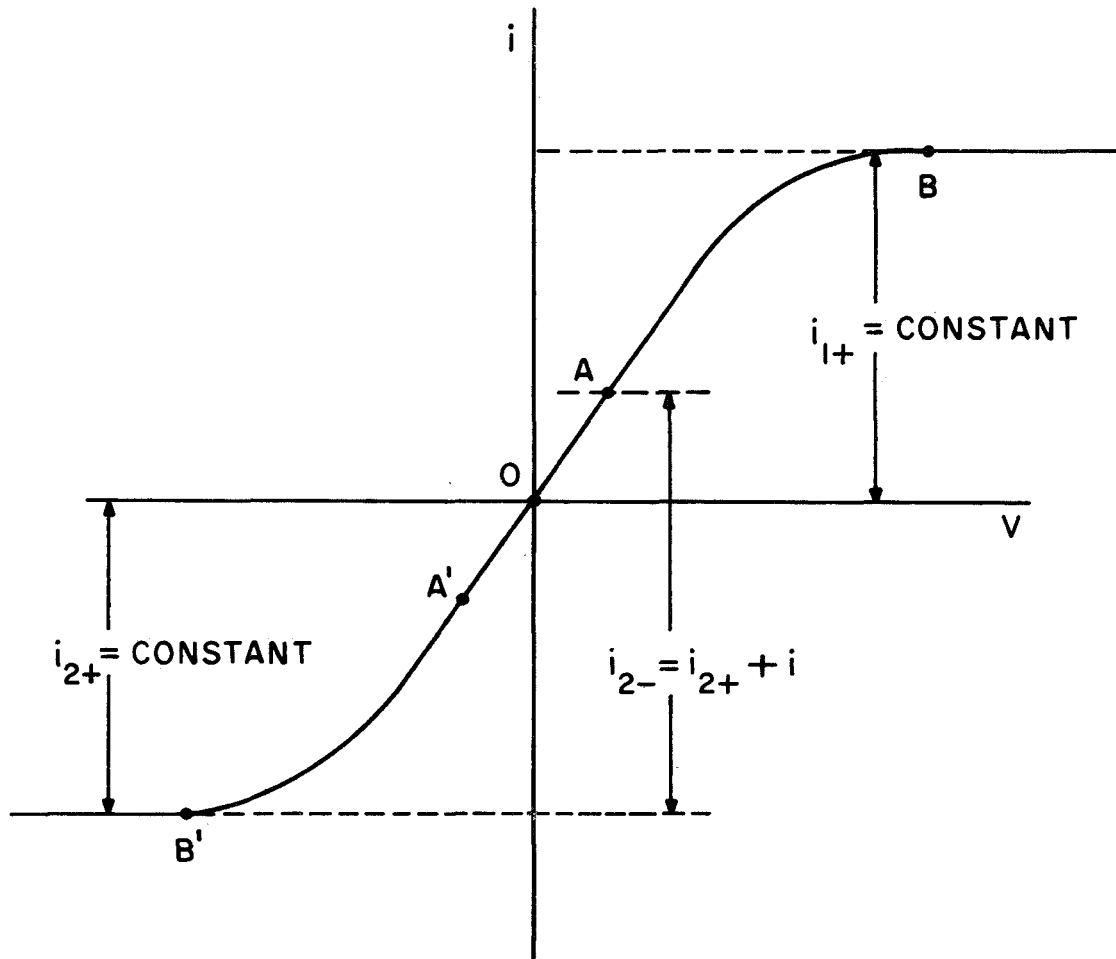
FIGURE 4

between the probes a current is drawn through the circuit. Neither probe is grounded and whole system "floats" with the space potential in the discharge plasma. By considering the differential voltage vs. current curves, the electron temperature and density of the plasma can be calculated.

Following the discussion of Johnson and Malter it is helpful in understanding the mathematical treatment of the problem if a qualitative description is given considering the behavior of the system in response to changes in the differential voltage.

The assumptions are made for simplicity that the probes have equal areas and that there is no contact or spacial potential differences between the probes. Since the practical voltages used are small it is also assumed that the differential voltage does not affect the ion current to the system.

First consider the case where the differential voltage is zero and no potential difference exists between the two probes. Since this is true there can be no net current in the loop. Both probes are floating at the same potential and drawing no net current from the plasma. This corresponds to the origin in Figure 5. The floating potential in this case is negative relative to the space or plasma potential. This can be justified by the following argument. The thermal velocities of the electrons are much greater than those of the ions while their densities are nearly the same (neutral plasma). Therefore more electrons per second will reach the probe than ions if there were no voltage on the



DOUBLE PROBE CHARACTERISTIC CURVE
(CURRENT VS VOLTAGE)

FIGURE 5

probe. The requirement that the probe draws no net current also requires then, that there be a voltage on the probe so that equal numbers of ions and electrons arrive. The floating potential in this case is thus negative relative to the space potential.

Now if the voltage difference is made slightly negative so that probe 1 is made more positive, then the potential of probe 1 would approach the space potential and that of probe 2 would move away from the space potential. Probe 1 is collecting more electrons while probe 2 collects less. The system would be located at point A in Figure 5.

When the differential voltage is made more negative the point is reached when most or all of the electrons arriving at probe 2 are repelled, and all the electron current is collected by probe 1. The potential of probe 1 is now near space potential. The system is located now at point B in Figure 5. Any further increase in the negative voltage between the probes produces no change in the currents. The potential of probe 1 remains near the space potential and that of probe 2 goes negative with the differential voltage. The system moves along the horizontal line left of point B in Figure 5. Probe 2 is said to be saturated with respect to positive ions. Probe 1 now collects sufficient electron current to balance the entire ion current flowing to the system.

In general it is found that the saturation current to a probe does not remain constant with respect to the change in voltage

when the system is moving to the left of B in Figure 5. This is attributed to the expansion of the sheath around the probe as the voltage becomes more negative. The curve then actually has a slope. However, it is small.

When the differential voltage is reversed and made more and more positive, the curve reaches points A and B in Figure 5. The curve is symmetric and the discussion holds with the interchange of the probes.

In the case at hand and in many instances the probe areas are not exactly equal. When this is the case the saturation ion currents to the probes are not equal. Likewise there is often a spacial gradient in potential between the probes. When this is true the curve does not pass through zero voltage. Neither of these effects cause error in the determination of the electron temperature.

a. Determination of the Electron Temperature

Continuing with the discussion of Johnson and Malter, if the system in Figure 4 is not grounded then Kirchoff's Law for a current loop becomes

$$i_{1+} - i_{1-} + i_{2+} - i_{2-} = 0$$

or

$$i_{1+} + i_{2+} = i_{1-} + i_{2-} \quad (24)$$

where "+" refers to the positive ions and "-" refers to the electrons. The currents are those to the respective probes as denoted in the subscripts. The same law applied to the voltages present indicates that

$$V_1 + V_c = V_2 + V_D \quad (25)$$

where V_1 and V_2 are the potentials of the two probes, V_D is the applied voltage, and V_c is the contact potential between the probe and the plasma. The contact potential may be extended to include any spacial gradient in potential between the probes due to the discharge field, or the position of the probes in the plasma. The last expression may be written

$$V_1 = V_2 + V_D - V_c \quad (26)$$

If the Boltzmann condition is used to relate the currents collected by the probes to the potentials on the probes, the following expressions are found.

$$i_{1-} = A_1 j_{o1} e^{-\phi V_1} \quad \text{and} \quad i_{2-} = A_2 j_{o2} e^{-\phi V_2} \quad (27)$$

where A's refer to the respective probe areas, and the j's refer to the random electron current reaching each probe, and $\phi = e/kT_-$.

Therefore,

$$i_{2+} + i_{1+} = i_{1-} + i_{2-} = A_1 j_{o1} e^{-\phi V_1} + A_2 j_{o2} e^{-\phi V_2}. \quad (28)$$

Dividing by i_{2-} and subtracting 1.0 from both sides,

$$\begin{aligned} \frac{i_{1+} + i_{2+}}{i_{2-}} - 1 &= \frac{A_1 j_{o2}}{A_2 j_{o2}} e^{-\phi(v_1 - v_2)} \\ &= \frac{A_1 j_{o1}}{A_2 j_{o2}} e^{\phi(v_c - v_D)} \end{aligned} \quad (29)$$

$$\text{Now let } \Gamma = \frac{i_{1+} + i_{2+}}{i_{2-}} - 1 \text{ and } \sigma = \frac{A_1 j_{o1}}{A_2 j_{o2}} e^{\phi V_c} \quad (30)$$

$$\text{Therefore } \ln \Gamma = \ln \sigma - \phi V_D \quad (31)$$

It is evident from this equation that the slope of a $\ln \Gamma$ vs. V_D plot is a measure of the electron temperature. Since σ contains the probe areas, electron random current densities and the contact potential, these quantities do not affect the slope of the plot and hence do not affect the calculation of the electron temperature. In fact the factors in σ do not show any explicit dependence on the plasma potential either.

In determining the errors present in the DPM, there are two main sources. First there is some uncertainty in determining the points B and B' in Figure 5. The estimation of the values of i_+

and i_{2+} introduces also a change in the estimation of i_{2-} in such a way that except near the knees of the curve, the value of Γ is not changed appreciably.

The second source of error is the fact that the ion currents to the probes may change with the voltage due to the variation in the sheath size around the probe. A thorough discussion of this is made by Johnson and Malter in the appendix of their article. The conclusions about this source of error are that, first of all, the value of $(i_{1+} + i_{2+})$ can hardly change appreciably over the region between the knees unless the slope of the saturation region has a large value. In any event Γ is not affected to any significant degree since $(i_{1+} + i_{2+})$ and i_{-} change in the same direction and in the same ratio. Secondly, the value of $(i_{1+} + i_{2+})$ remains constant since a change in i_{1+} tends to be compensated for by an opposite change in i_{2+} . It can be seen that it is not necessary to compute the ion currents over the whole range between the knees of the curve to avoid this error.

Since the system in Figure 4 floats with respect to the space potential, and the potential of the probe is always somewhat negative by comparison, only a small fraction of the electrons in the distribution are sampled. Only the electrons with energies great enough to surmount the potential barrier are collected by the probes. For example in Argon at 1 Torr, Johnson and Malter calculate that less than one percent of the electron distribution

was sampled in one particular case in their analysis. This fraction can be increased by using probes with highly unequal areas.

b. Determination of the Plasma Density

The second important plasma parameter is the density of charged particles. Once the electron temperature has been found the density can be calculated. The assumption is made that $n_+ = n_- = n$. The random ion current density to the probe can be written

$$j_+ = n_+ e \bar{v}_+^{\text{drift}} \quad (32)$$

where \bar{v}_+^{drift} is the average drift velocity of the ion. Thus the random ion current to the probe is

$$i_+ = A_s j_+ = A_s n_+ \bar{v}_+^{\text{drift}} e \quad (33)$$

where A_s is the area of the ion sheath around the probe.

Therefore

$$n_+ = \frac{i_+}{A_s e \bar{v}_+^{\text{drift}}} \quad (34)$$

The usual procedure from here is to find the area of the sheath from an expression relating the floating potential to the radius of the sheath. The expression for the space charge limited current to a diode relates these two quantities. From Johnson and Malter,

$$i_+ = 14.66 \times 10^{-6} \left(\frac{m_-}{m_+} \right)^{1/2} \frac{LV^{3/2}}{a\beta^2} \quad (35)$$

where L is the length of the probe, and V is the potential drop from the probe to the plasma. The dependence of the current on the sheath radius is contained in the function β^2 . This expression relates the potential difference with the function β^2 . The problem now is to determine the value of this potential difference. The floating potential relative to the space potential can be expressed as

$$V_F = - \left(\frac{kT_-}{2e} \right) \ln \left(\frac{T_- m_+}{T_+ m_-} \right) \quad (36)$$

If we consider the change in electron current to probe 2 as the circuit current moves from zero to the saturation value the following expressions are evident.

$$\frac{i_{2-}^{(o)}}{i_{2-}^{(s)}} = \frac{A_2 j_{o2}}{A_2 j_{o2}} e^{\phi(V_s - V_F)} \quad (37)$$

where V_s is the probe-space potential at saturation. Therefore letting $\Delta V = V_s - V_F$ we have

$$\frac{i_{2-}^{(o)}}{i_{2-}^{(s)}} = e^{\frac{e\Delta V}{kT_-}} \quad (38)$$

The change in i_{2-} can be calculated from the $\ln \Gamma$ vs. V_D curve and hence ΔV can be found. Then we know

$$V = |V_F| + \Delta V \quad (39)$$

With this value of V at saturation we can find β^2 and the sheath area. The functional relationship between β^2 and the sheath radius is given by Langmuir and Compton (1931). This dependence is plotted in Loeb (1939, p.323). Since the sheath around the probe acts as a virtual emitter, the $(-\beta^2)$ curves of Loeb should be used.

5. Double Probes, $B \neq 0$

The case of double probes in a magnetic field can be treated in much the same way as the single probe in the magnetic field. This is true because in the double probe method, both saturation currents are ion currents. That is, the knees in the current vs. voltage plots are caused by ion saturation of the probes, in contrast to the single probe case where there is a knee for both electron and ion saturation.

The problem becomes then a study of the effect of a magnetic field on the saturation ion current to a probe. The important difference in the theories for ion collection in a

magnetic field becomes apparent when the condition that the Larmor radius for the ions is much greater than the probe radius, is violated.

Knechtli and Wada (1961) used double probes in a magnetized Cs plasma with some success when the magnetic field was kept below a certain critical value. Sugawara and Hatta (1965) in two papers treated the problem of the validity of the DPM in a magnetic field. A short summary of their work will be given.

When $a \gg l_{\perp}$, the probe depletes the surrounding space of electrons. More electrons are collected than can be supplied to the area by diffusion. This is especially true in a magnetic field since diffusion across the field is reduced. Bohm (1949) assumed that current to the probe in a magnetic field could be attributed to 1.) the random thermal current, and 2.) the electric field and diffusion that direct the current toward the probe. Diffusion will be important when $l_D \ll l_{\perp}$. Bohm shows that the drift due to the electric field when $T_+ \ll T_{\perp}$ can be neglected. Therefore with the assumption that the depletion can be made up solely by diffusion, and that the diffusion equation can be used up to the probe surface, the quantities I_{\perp} and I_{\parallel} were derived by Sugawara and Hatta. For plane probes,

$$I_{\perp} = D_{\perp} \int \nabla n \cdot dS_x \quad (40)$$

where ds_x is the surface element of the probe in the y-z plane.

The solution found by Sugawara and Hatta is

$$\frac{I_{\perp-}}{I_{o-}} = \frac{\pi}{2K(k)} \alpha^{1/2} \frac{1 + 32/3 \left(\frac{1_{o-}}{\pi a P} \right)}{1 + 16/3 \left(\frac{1_{o-}}{K(k) a P} \right) \alpha^{1/2}} \quad (41)$$

$$\frac{I_{||-}}{I_{o-}} = \alpha^{1/2} \frac{1 + 32/3 \left(\frac{1_{o-}}{\pi a P} \right)}{1 + 16/3 \left(\frac{1_{o-}}{\pi a P} \right) \alpha^{1/2}} \quad (42)$$

and

$$\frac{I_{\perp-}}{I_{||-}} = \frac{\pi}{2K(k)} \frac{1 + 32/3 \left(\frac{1_{o-}}{\pi a P} \right) \alpha^{1/2}}{1 + 16/3 \left(\frac{1_{o-}}{a P K(k)} \right) \alpha^{1/2}} \quad (43)$$

$$\text{where } k = (1-\alpha)^{1/2}, \quad \alpha = (1+\psi^2)^{-1} \text{ and } \psi = \omega\tau \quad (44)$$

and ω = the cyclotron angular frequency, τ = the mean collision time and $K(k)$ = the complete elliptic integral of the first kind. To discuss ion collection now, Sugawara and Hatta made the assumption that in finding the limiting critical field the effect of the

magnetic field on the saturation ion current would be the key. They also assumed that the ion sheath thickness could be neglected in comparison with the probe radius when using equation (41) to find the critical field. By substituting l_{o+} for l_{o-} in the preceding equation, the following result was obtained.

$$\frac{I_{\perp+}}{I_{o+}} = \frac{\pi\alpha^{1/2}}{2K(k)} \frac{1 + 32/3 \left(\frac{l_{o+}}{\pi a P} \right)}{1 + 16/3 \left(\frac{l_{o+}}{aPK(k)} \right)} \quad (45)$$

To determine the critical field, they plotted $I_{\perp+}/I_{o+}$ vs. $\omega_{+}\tau_{+}$. The result was that the ratio $I_{\perp+}/I_{o+}$ was affected by the magnetic field when $B = 800$ gauss.

If one makes the substitution l_{o+} for l_{o-} in equation (43) the result is

$$\frac{I_{\perp+}}{I_{||+}} = \frac{\pi}{2K(k)} \frac{1 + 32/3 \left(\frac{l_{o+}}{\pi a P} \right) \alpha^{1/2}}{1 + 16/3 \left(\frac{l_{o+}}{aPK(k)} \right) \alpha^{1/2}} \quad (46)$$

II. EXPERIMENTAL APPARATUS AND PROCEDURES

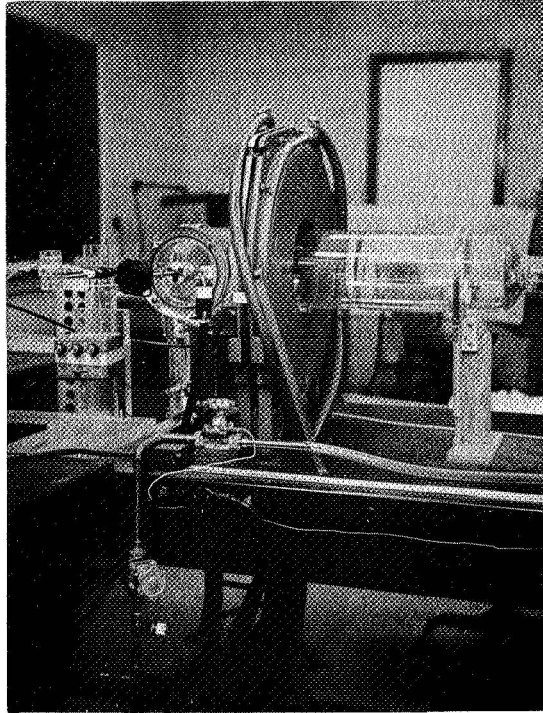
A. Apparatus

1. Supporting Equipment

The main systems of experimental instrumentation used in this study are the probes and the supporting equipment including the discharge and the magnet. The discharge was created by high voltage breakdown of the gas in the main discharge tube. The tube and its supports are shown in Figure 6. To produce the discharge, the pressure was reduced to the desired level by a mechanical roughing pump. A large potential difference was created between the grounded aluminum anode and a coiled tungsten wire cold cathode, located 71.5 cm. away. The glow discharge thus formed included a positive column which filled nearly half of the tube under typical operating conditions like $V=1.5$ kV, $I=15$ mA, and $P=1.0$ Torr.

The diameter of the main tube was 14.4 cm. (ID) and that of the side tube was 11.5 cm. (ID). The aluminum anode was a disk .64 cm. thick and 7.6 cm. in diameter. The cathode was constructed of coiled tungsten filament wire, the diameter of the coil being 1.5 cm.

The measurements of the conditions in the positive column were taken at two different pressures. The pressure was measured with a diaphragm-type gauge which had been calibrated in the range 0-2 Torr by a Hastings vacuum gauge. Nitrogen and air were both used at .2 and 1.0 Torr.

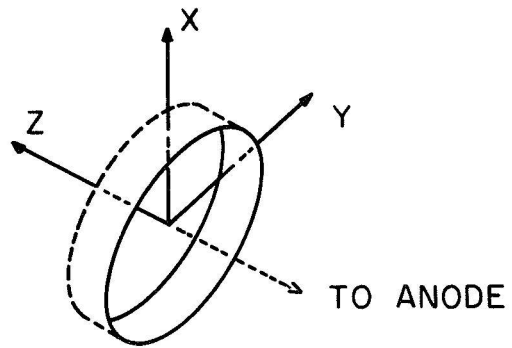
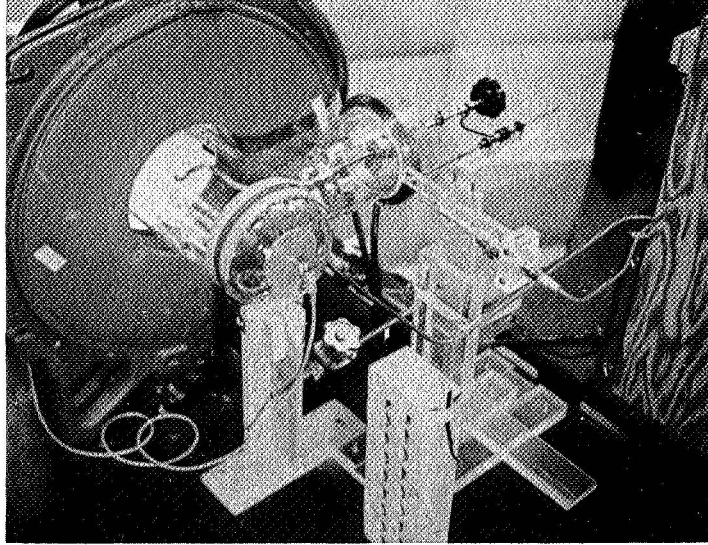


EXPERIMENTAL APPARATUS

FIGURE 6

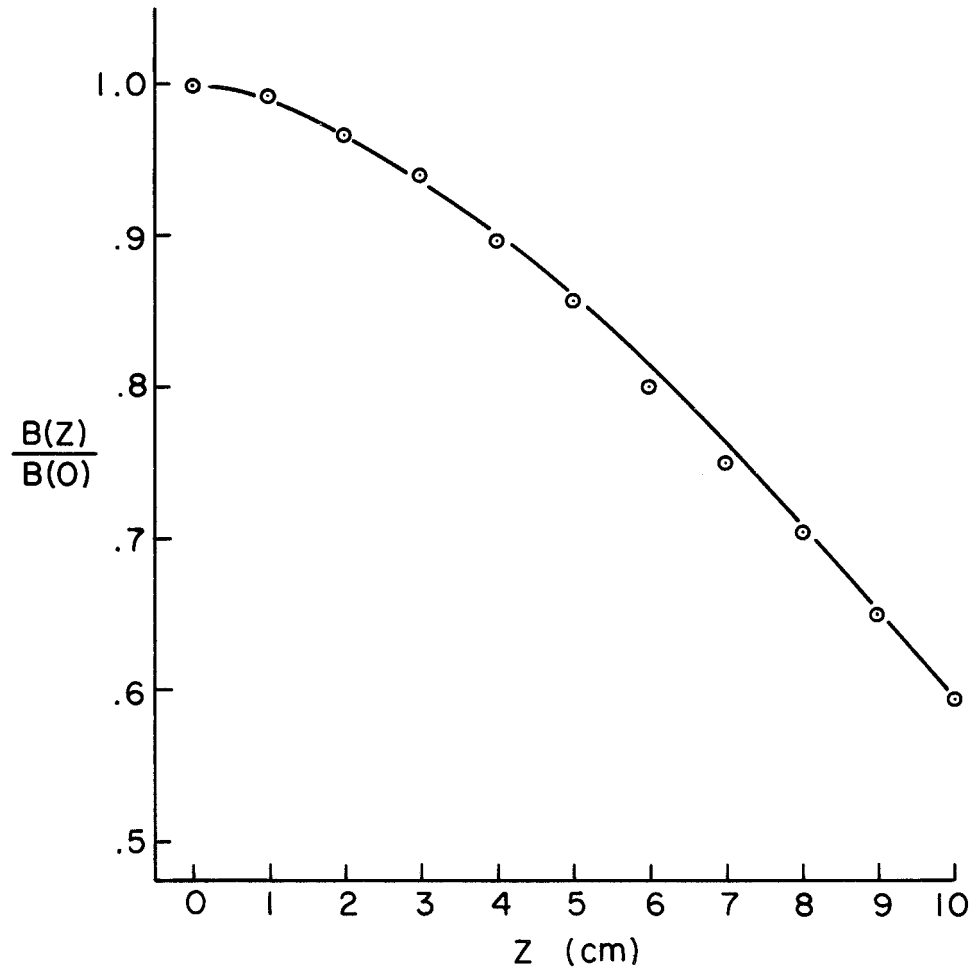
To produce the magnetic field a circular water-cooled electromagnet was placed around the discharge tube as shown in Figure 7. The coil had a small number of turns, so large currents were needed to produce the field. In the central hole of the magnet the field ranged from 0-3,000 gauss, but fields of 200 gauss were the largest used since instabilities in the discharge itself resulted when higher fields were used. The central hole was 7.6 cm. thick and 17.8 cm. in diameter as shown in Figure 7. It should be mentioned here that the center of the hole served as the center of the co-ordinate system used throughout this study. The co-ordinate system is indicated in Figure 7.

The magnetic field was mapped for various axes parallel to the z-axis in 1.0 cm. steps up to 10 cm. from the center of the hole. Gaussmeters made by Bell Inc. and Empire were used to map the field, and a differential probe was used with the Bell Gaussmeter to measure the gradients of the z-component of the field. The measurements were made with the probe mounted on a plexiglass device which was adjustable in three dimensions. To insure reproducibility, the device was rigidly mounted on the supporting table. The magnitudes of the field and the gradients present in the central hole of the magnet are shown in Figures 8 and 9.

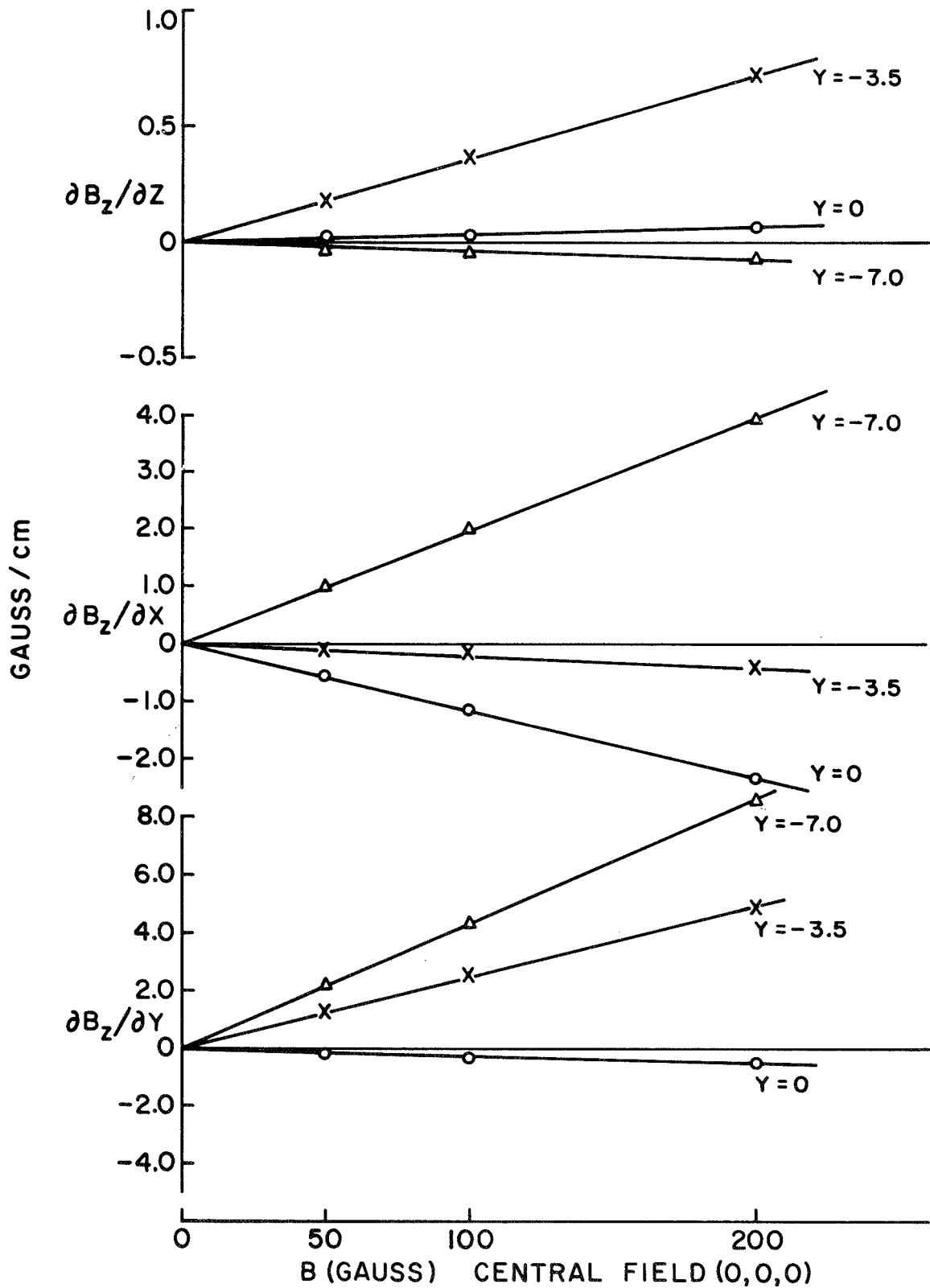


DISCHARGE TUBE, MAGNET
AND CO-ORDINATE SYSTEM

FIGURE 7



MAGNETIC FIELD ON THE Z AXIS
FIGURE 8



GRADIENT OF B_z VS RADIAL POSITION AND
MAGNETIC FIELD
FIGURE 9

The Empire gaussmeter was calibrated so that the field at the origin of the co-ordinate system could be monitored although the gaussmeter probe was external to the discharge tube. Both gaussmeters were needed to make this calibration. The probe that was monitoring the field was then rigidly attached to the supporting table.

The current for the magnet was supplied by a DC generator and the following expression gives the magnitude of this current in the range 0-500 gauss.

$$I = cB \quad \text{where } c = .275 \text{ amps/gauss}$$

$$B \text{ [gauss]}$$

$$I \text{ [amps]} \quad (47)$$

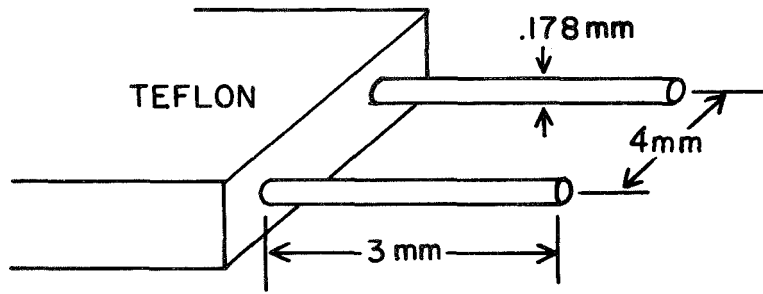
The double probe characteristics (current-voltage plots) were taken point-by-point using a precision voltmeter and a Boonton Inc. Sensitive DC meter to measure the current. The voltage source for the probes was a Kepko power supply (0-2500 volts, 2 mA). Although a very high voltage device, the fine adjustment on the power supply was sufficiently sensitive to permit the use of 5 volt increments. To protect the probe leads from electric field effects they were shielded with the outer conductor of a large diameter co-axial cable. This shield was extended into the discharge tube and covered the internal leads up to within approximately 5 cm. of the probes.

2. The Probes

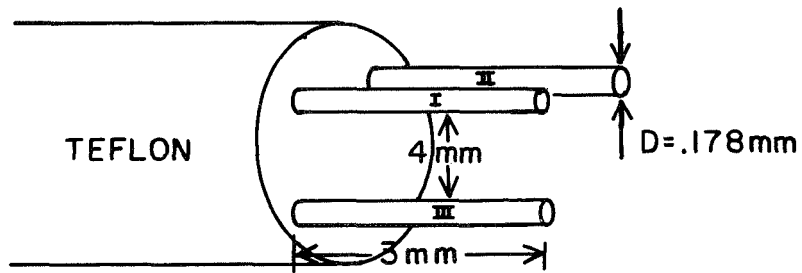
The last important system in the experimental instrumentation is the probe sets. Figure 10 is sufficient to describe their geometry, but a brief description of the construction methods will be given.

The first set of two probes were mounted in a small teflon block, being separated by 4 mm. The probes were 3 mm. long and .178 mm. in diameter (7 mil tungsten wire). The probe assembly was mounted on the end of a rotary push-pull feedthrough to permit radial measurements to be taken. The radius would then correspond to the $\pm y$ directions. The z co-ordinate of this radius was -12, 10 cm. from the anode. All measurements taken with the first two sets of probes were taken at this position on the z-axis.

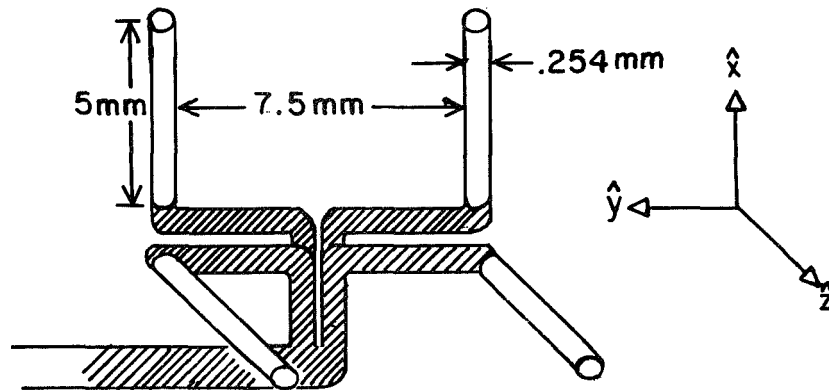
The second set of probes was made of the same diameter tungsten wire. The dimensions are given in Figure 10. Of the three probes seen, two adjacent probes were used in turn as a double probe, each set having different relative positions. For example, Probes I and II were one set and probes I and III the other. The teflon cylinder in which these probes were mounted was oriented in such a way that the one pair of probes had common x and y co-ordinates, but the other set had common y and z co-ordinates. The first orientation was used to obtain measurements of any wake effects that might arise in a magnetic field when one probe is "downstream" from the other. The second was to obtain measurements to correlate with the other case. These three probes were mounted



A. PROBE SET NO. ONE



B. PROBE SET NO. TWO



C. PROBE SET NO. THREE

DESCRIPTION OF THE PROBES

FIGURE 10

on the end of the feedthrough in a manner similar to the first set of probes.

The last set of probes consisted of two pairs of double probes, the planes of which were perpendicular to one another. A somewhat larger diameter tungsten wire was used (10 mil.), and the probes were constructed in a different way. Instead of inserting the wires into small holes in teflon mounting, these were shaped to the desired geometry and fastened together with epoxy resin. The wires were insulated with regular plastic insulation up to their common apex. Continuing from that point, an epoxy resin covering insulated the wires excepting the 5 mm. of the wire tips which acted as the probes.

The particular geometry shown in Figure 10 was chosen to avoid any wake effects which might arise in the presence of a magnetic field. As shown in the figure, both sets had common x and z coordinates with different y positions. The pair that were parallel to the z-axis were assumed mainly to collect current across the magnetic field. The pair that were parallel to the x-axis were assumed to collect current mainly along the field lines. The degree to which these assumptions prove true will be discussed later.

In order to place the probes at the center of the hole in the magnet, they were mounted on an "L"-shaped extension of the feedthrough. The shortest leg of the "L" ran parallel to the z-axis along the side of the tube. It is visible in Figure 7. The leads were shielded with braided copper wire to assure the exclusion of

any electric field perturbations of the probe current. When the probes were mounted in this fashion they were at the center of the hole in the magnet and on the axis of the main tube, the origin of the co-ordinate system. At this point the anode was 22 cm. along the $-z$ axis.

B. Procedures

The glow discharge illustrated in Figure 1 is only characteristic of the gas discharge within a certain current, voltage and pressure range. The measurements of this study were made under conditions such as $I=10-30$ mA, $V=1.0-2.5$ kV, and $P=.2-1.0$ Torr in air and in pure nitrogen. Striations occurred in air for pressures below those mentioned above, and in both the air and pure nitrogen, instabilities occurred when high currents (and voltages) were used.

The procedure for obtaining a certain pressure was to evacuate the system as much as possible and then to bleed in the desired gas until the operating pressure was reached. When nitrogen was used, this process was repeated several times, bleeding in nitrogen until the pressure rose to 40-50 Torr, then pumping the system down again. This procedure was used to help insure that the tube contained a very high percentage of nitrogen and a very low percentage of other gases. All of the conditions were adjusted to make the discharge as stable as possible for the range of magnetic fields that were used.

The magnetic field at the origin of the co-ordinate system was monitored by an external gaussmeter probe. Once the magnetic field control was set to give a specific reading by the probe, from previous calibration, the central field was known. This method was found to be somewhat easier than measuring millivolts across a 50 mV/1 kA shunt resistor in the circuit with the magnet. The probe was calibrated with a 860 gauss standard magnet before each set of

Figure 6 shows the position of the magnet relative to the anode and cathode, from which it is evident that the magnetic field could be considered uniform only over a short distance. To help to understand the nature of the field, the following description of the magnet is given. The magnet was made of two coils of copper bus-bar approximately 5/8 inch by 1/8 inch placed side-by-side. The current moved through one coil from the outside rings toward the center, across a cylindrical conductor into the central rings of the other coil and proceeded toward the outside.

The analytical expression for the magnetic field due to this magnet was not expressed. A more simple approach was taken that the measured gradients would give an equally revealing description of the possible causes of the effects which would alter the characteristics of the discharge from those of a discharge in a uniform field.

The double probe current-voltage curves were taken point-by-point in 5 volt intervals. To reverse the terminals of the voltage source a double-throw double-pole switch was used. Probe sets Nos. 2 and 3 required extra switches to select the proper pair of probes when measuring parallel and perpendicular to the z-axis. After the proper discharge conditions were achieved the voltage between the probes was applied in 5 volt increments and the corresponding currents were recorded. Three different but equivalent methods of collecting this data point-by-point were used to check their equivalence. First, the positive potential difference was applied between the probes in steps and the currents recorded. Then the negative part of the curves were plotted for the same set of probes. Secondly, the positive voltage was selected and different double probe sets were used at each increment. Thirdly, the voltage between a given set of probes was switched from the positive to the negative sense. The first method was most frequently used as the selector switch on the ammeter needed to be changed less often. As mentioned earlier, the three methods were equivalent.

When the magnetic field was applied, several effects were apparent which were not necessarily desirable. Beside the radial collapsing of the column which was expected, the length of the column was affected also. As the field was monotonically increased to approximately 250-300 gauss, the column was shortened. However, as the field was increased further to the 600-700 gauss level, the

column was lengthened. To avoid this change in length, the magnetic field was limited to the lower range at all times, and the probes were always kept well within the glowing column.

Another effect of the field was on the stability of the discharge. The current and voltage were made at times to oscillate slowly by the application of a strong field. The oscillations were clearly visible and were eliminated again by restricting the upper value of the magnetic field to 300 gauss.

Consider now the positions along the z-axis where double probe measurements were made. The co-ordinate system is illustrated in Figure 8, and the probes are shown in Figure 10. All of the measurements by the first two sets of probes were made at $z=-12$ cm. and $x=0$. The y position was varied to make radial measurements by moving the feedthrough. The measurements of probe sets 1 and 2 were made in air at .2 Torr, and nitrogen at 1.0 Torr.

Probe set number 1 was used mainly to obtain measurements for probes at two different z positions. The second set of probes were used to collect measurements of possible wake effects arising when two probes are placed side-by-side in a magnetic field. When two probes are in this orientation, one of them is in a direct line to block or partially block the collection by the other probe of particles drifting along lines parallel to the z-axis. When there is no magnetic field, this effect would be reduced since particles arrive at the collecting probe from all directions, none being preferred. In a strong magnetic field, however, the motion of the

particles is restricted to paths parallel with the magnetic lines of force, hence, a probe may cast a "shadow" on the region immediately "downstream" by blocking the path of particles approaching along these paths. The stronger the magnetic field the more pronounced this effect would be.

Probe set number 2 was used in both the side-by-side and one-above-the-other orientation on the z-axis and 2 cm. off the axis at $y=2$ cm. in nitrogen at .2 Torr. Note that current collected by the probes when in either of these two orientations arrives mainly along paths parallel to the magnetic lines of force.

In contrast, current collected by probe set 3 was from directions both parallel and perpendicular to the magnetic field. This set of probes was used to study the effect of the magnetic field on the plasma parameters on the z-axis in nitrogen at 1.0 Torr. The effect of the magnetic field on the DPM was (in this fashion) also studied by probe set number three.

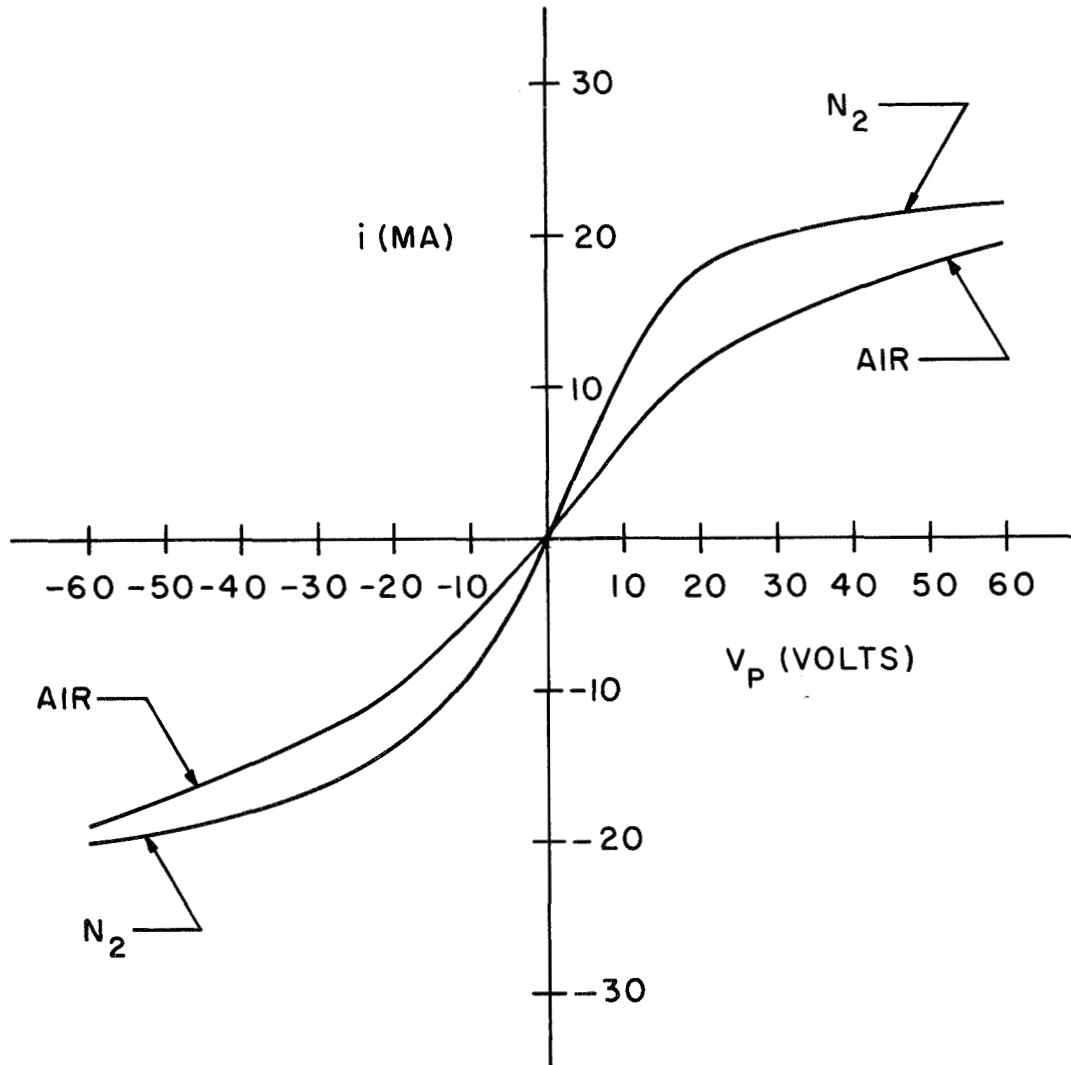
III. RESULTS AND DISCUSSION

A. The Positive Column, $B=0$

The first case is the positive column with no applied magnetic field. Figure 11 is a comparison between the measurements made by probe set number 1 in air and those in pure nitrogen at .2 Torr. In both cases and in all of the double probe measurements, the DPM of Johnson and Malter (1950) was used to find the electron temperature and density.

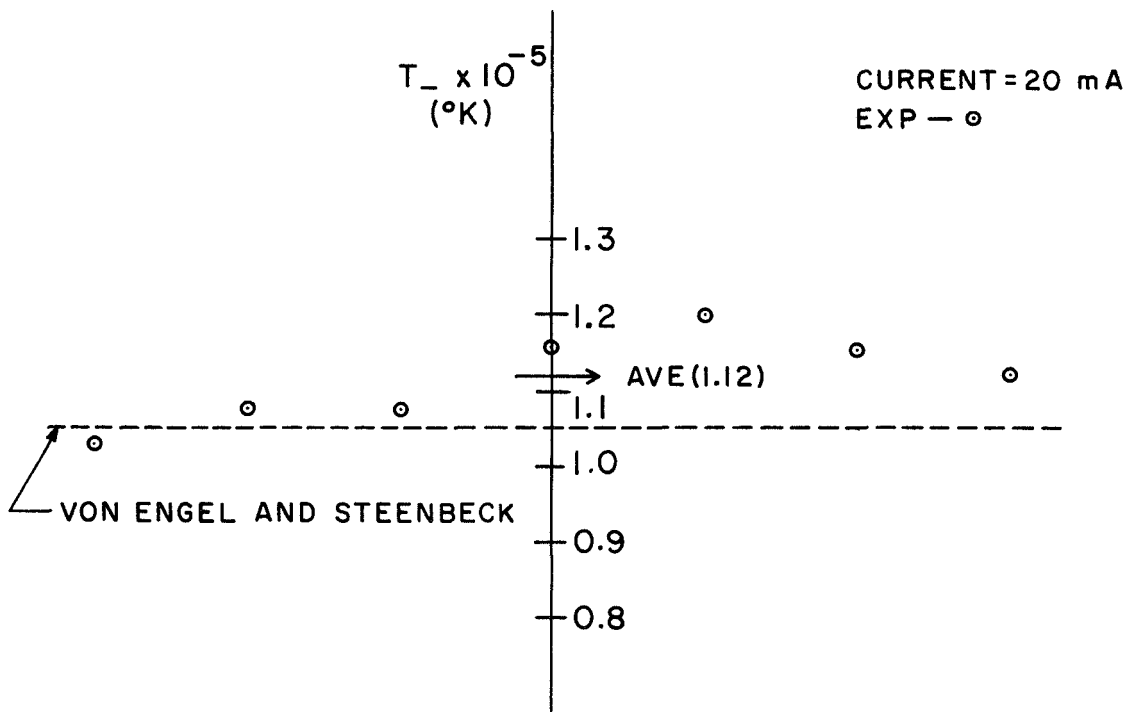
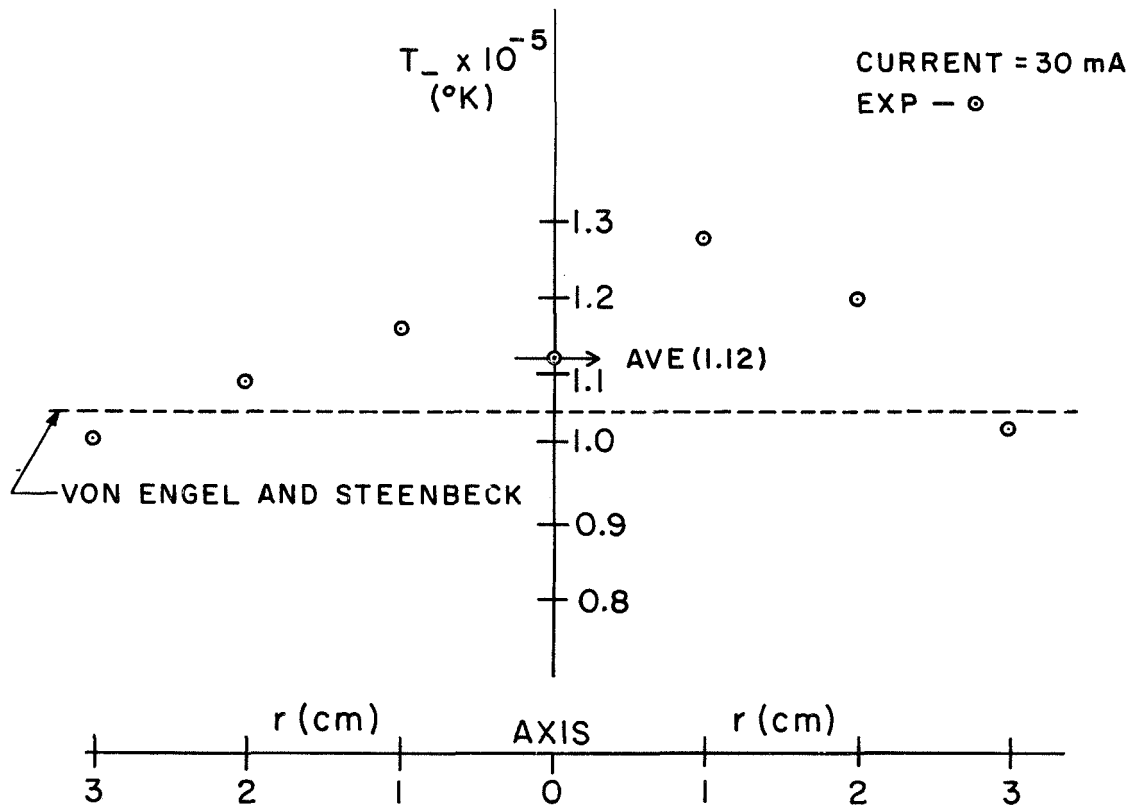
The figure shows that saturation of the probes is somewhat destroyed in air, i.e. the knees of the curve are less distinct than they are in nitrogen. The position of the knees depends on the mass of the ions being collected, so that the position would shift if the change from air to pure nitrogen were made. The exact reason why the knees are not distinct in air is not clear. Electron temperatures calculated from the data collected in air show that although the data is reproducible, the variation from the mean value is greater than should be expected. This error is attributed to the estimation of the slope and position of the knees of the curves.

As previously mentioned typical measurements of probe set number 1 in nitrogen at .2 Torr are illustrated in Figure 11 labeled N_2 . The radial variation of the electron temperature calculated from these data is found in Figure 12 for two different discharge currents. According to the theory of the positive column

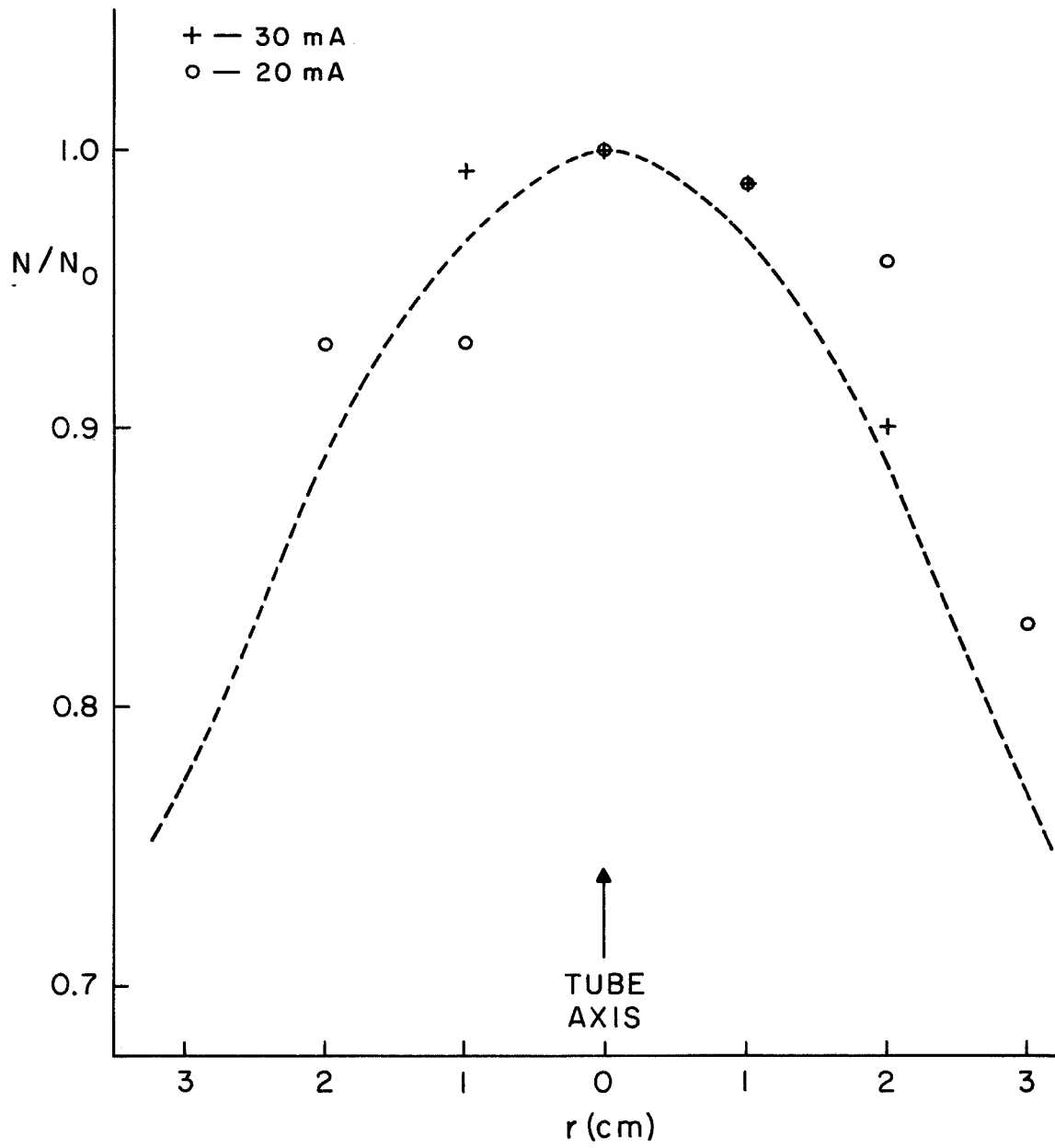


TYPICAL CURRENT VS VOLTAGE CURVES FOR
AIR AND N_2 (PROBE SET NUMBER ONE)

FIGURE II



ELECTRON TEMPERATURE VS RADIUS
FIGURE 12



RELATIVE DENSITY VS RADIUS
FIGURE 13

the temperature profile is a constant across the tube. Figure 12 shows that within approximately 15 percent this profile is a constant. The limit of the experimental error of the method was estimated to be about this large, so the temperature can be assumed to be constant across the tube. The average value of the temperatures calculated for points near the central axis of the tube is 1.12×10^5 degrees K. for both currents.

In the same figure, the electron temperature calculated from the theory of von Engel and Steenbeck (1932) is indicated by a broken line, $T = 1.05 \times 10^5$ degrees K. The agreement between theory and experiment is good (within 10 percent).

At this point the reason for excluding temperature measurements near the walls of the tube should be given. When measurements were taken at radii equal to or greater than approximately 4 cm, the temperatures and densities derived from these values proved to be inconsistent with the data collected near the axis. The values of the temperature were not symmetric on either side of the axis, and the densities were unusually high. The reason for these spurious data was attributed to an interaction by the probes with the processes occurring near the walls. For the same reason density measurements near the walls were not included in the following discussion.

Using the data collected by probe set number 1, the radial variation of the relative plasma density was calculated and is shown in Figure 13. Recalling the theory of Schottky, (1924, 1925)

the figure indicates that near the tube axis the experimental values agree with the theory or are very close to it. In the figure, the Bessel function of order zero is the broken line.

To make the DPM of Johnson and Malter (1950) clear, the electron temperature and density of a sample set of data are calculated in the Appendix. The data was collected by probe set number 1 at (0, 1, -12) in nitrogen at 1.0 Torr. See the Appendix for the current vs. voltage and the $\ln I$ vs. V plots.

To check if the drift of particles due to the longitudinal electric field affected the double probe measurements, probe set number 1 was moved in the plasma so that it assumed all orientations with respect to the axis of the tube. These measurements were taken in nitrogen at 1.0 Torr at the position mentioned previously. In both parallel and perpendicular orientations with respect to the tube axis, the electron temperatures and densities were the same within the experimental error.

B. The Positive Column, $B \neq 0$

When the magnetic field was applied to the positive column the resulting information was collected by probe sets 2 and 3. Probe set number 2 was used to indicate whether a wake effect did occur in the magnetic field. As explained before, when the particles in the column have on the average a drift due to either the electric field or a restriction on the random motion, then two probes placed close together may affect the collection of ions by each other. Data collected at (0, 0, -12) indicated that

$T_w/T_o = .7$ and $N_w/N_o = 1.0$ where the subscript "w" means wake or a quantity which was measured by two probes oriented in such a fashion that they could possibly interfere with one another, and the subscript "o" means those quantities measured by probes very unlikely to interfere with one another.

At (0, -2, -12) the ratios changed to $T_w/T_o = .8$ and $N_w/N_o = .8$. The ratios of the electron temperatures indicate that there was some interference in estimating the temperature with probes whose common plane was parallel to the magnetic field.

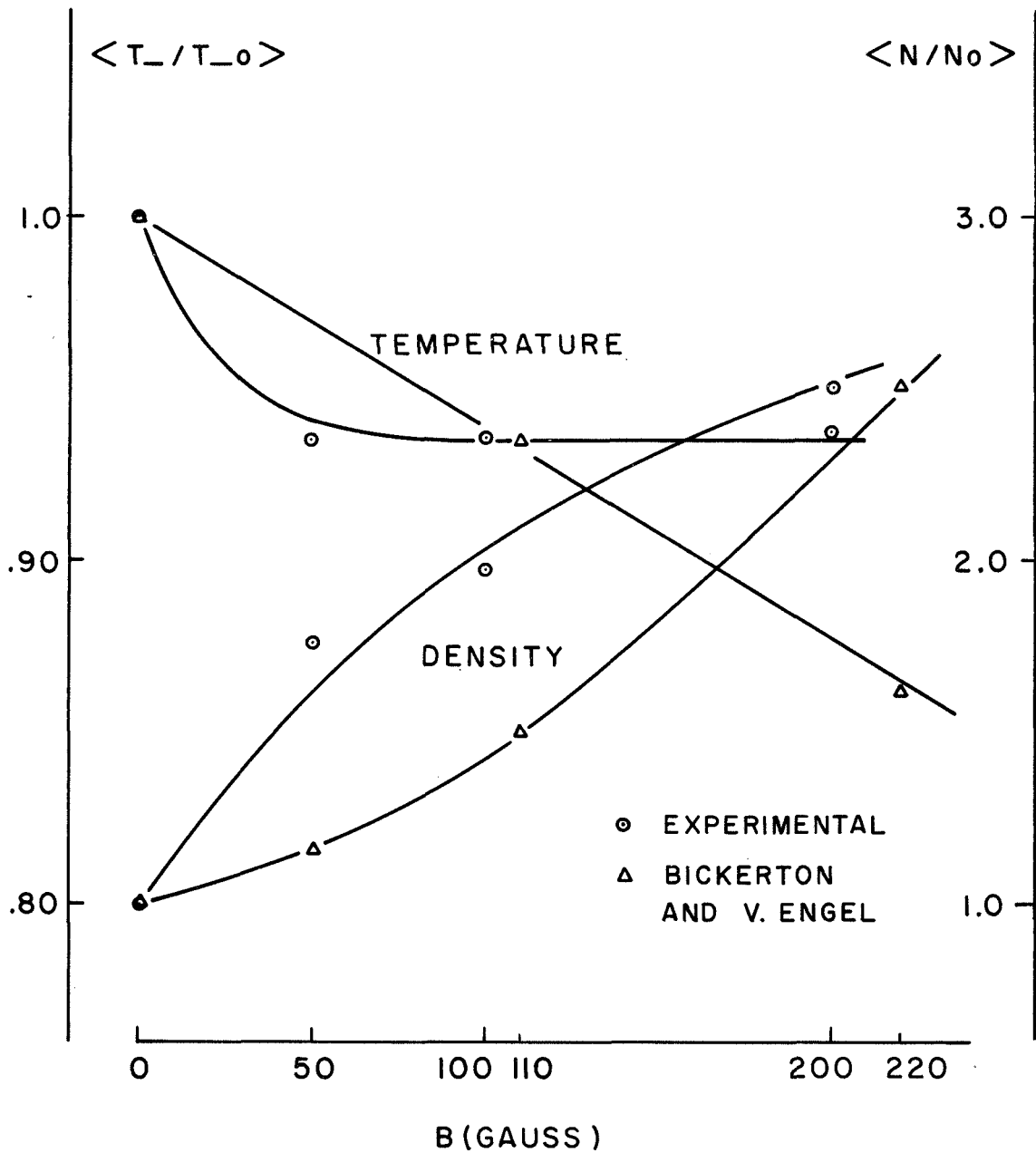
The measurements also indicated that although the plasma density estimate was different, the change was not as great. The determination of the density by the DPM of Johnson and Malter seems to be somewhat insensitive to this type of interference by the probe orientation. There is no theory which would allow a comparison for measurements taken in the wakes of objects, but these measurements do indicate that there is interference especially in estimating the electron temperature. At any rate the best orientation for a double probe set in a magnetic field is with the common plane perpendicular to the field for collection along the field lines, and with the probes parallel with the field for collection across the field lines. This is the scheme which was used with probe set 3 in measuring the changes in electron temperature and density on the axis in a variable magnetic field.

Now consider the measurements made by probe set 3 on the axis of the discharge tube at (0, 0, 0). Figure 14 illustrates the effect of the magnetic field on the electron temperature and density calculated from data collected in nitrogen at 1.0 Torr.

In the figure, the measurements of Bickerton and von Engel (1956) are shown. They represent the positive column of a helium discharge at .048 Torr and in a tube of radius $R=1.8$ cm. The experimental curve of this report was calculated in a tube of radius $R=7.2$ cm. The temperature $T_{-}=T(B)$ and $T_{-0}=T(0)$. Likewise the density $N=N(B)$ and $N_{0}=N(0)$. The ratios are an average of the measurements taken by both orientations of the probes in set number 3 for a given magnetic field.

One point should be made in comparing the curves in Figure 14. The work of Bickerton and von Engel was done at .048 Torr, in a dilute plasma. When the pressure is as great as 1.0 Torr, the plasma in nitrogen was approaching that of the continuum case. It is difficult to tell then, whether the differences noted on the curve are due to pressure, non-uniform magnetic field or an effect on the method of measuring. However, it can be seen that the electron temperature decreases more rapidly than that indicated by Bickerton and von Engel and then levels off instead of continuing to decrease.

The density ratios of this experiment tend to increase more rapidly than those of Bickerton and von Engel but show the same general slope for higher fields. The curves indicate that the density on the axis in both cases seems to rise in roughly the same fashion.



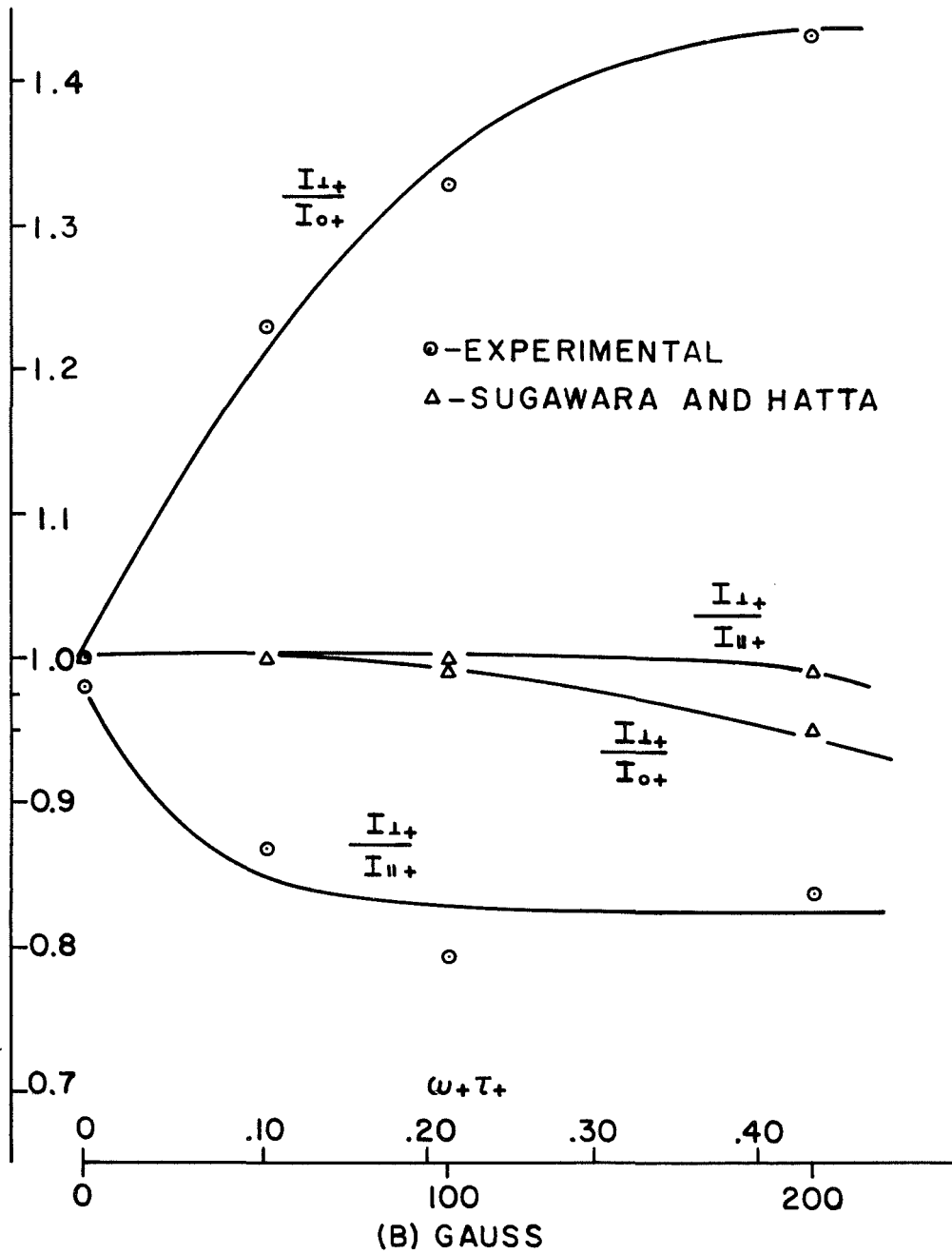
RELATIVE ELECTRON TEMP
AND DENSITY VS MAGNETIC
FIELD

FIGURE 14

Another indication of the effect of the magnetic field on the plasma can be observed by the change in the saturation currents to the probes. Sugawara and Hatta (1965A) derived an expression for the ratio of electron saturation current collected perpendicular to the field--to the electron saturation current for $B=0$. The ratio is given by equation (41). This expression was later extended to include the ion saturation currents given by equation (45). Figure 15 indicates these quantities and those in equation (46). The ratio in equation (46) is the ion saturation current collected perpendicular to the field divided by the saturation current collected parallel with the field for the same magnitude, not for zero field as is the denominator of equation (45).

The theory of Sugawara and Hatta was supported by experiments using plane double probes in neon at .5 Torr, with various combinations of positions for the probes. The present study employed cylindrical probes only, being parallel to each other, and equidistant from the anode of the discharge.

The theoretical values of the ratios in the figure are the solid lines, and can be seen nearly constant for fields under 100 gauss. The experimental points representing an average of the measurements are connected by the line labeled EXP. The ratio $I_{\perp+}/I_{0+}$ (exp.) increases rapidly for fields below 100 gauss and levels off near 200 gauss. The difference noted between this curve and the theory for plane probes can be due to various effects. Firstly, the probes used were cylindrical, not plane. Secondly,



SATURATION ION CURRENTS
 VS MAGNETIC FIELD

FIGURE 15

the pressures were a factor of 2 different, and thirdly, the theory neglects the ion sheath size relative to the probe radius. In our case, the ion sheath was estimated to be several times the probe radius.

The ratio $I_{\perp+}/I_{\parallel+}$ is perhaps a better indication of the effect of the magnetic field on the saturation current since the effect of the changing density is excluded from it by considering two values of the current at the same magnetic field. The ratio is shown to decrease and level off near 100 gauss. The theoretical ratio decreases very slowly for low fields and was used by Sugawara and Hatta to determine the field above which they considered the DPM unreliable. The experimental curve indicates that in the type of field used in this case the method is affected at much lower fields, if the assumption is made that the curve is independent of factors such as pressure, geometry of the probes, and the size of the ion sheath.

IV. SUMMARY

A study of a magnetized cylindrical positive column of a nitrogen glow discharge was presented. The study was made via the floating double probe method of Johnson and Malter (1950), single probes being ruled out because they collected a large fraction of the total discharge current under the operating conditions. A discussion of the single probe theory was included since the saturation of a probe in the double probe method is similar in certain aspects to the single probe.

The glow discharge was described in general terms, including a brief qualitative treatment of the various glow and dark regions of the discharge. The main emphasis was placed upon the positive column of a cylindrical discharge with and without a uniform magnetic field. Since the theory of a discharge in a non-uniform magnetic field is not complete to date, the nature of the field and its gradients were noted, but the theory of a uniformly magnetized column was applied.

It was the original intent that the effect of the non-uniform magnetic field on the double probe method could be derived from this study, but the fact that the positive column in a non-uniform field is not completely understood precluded the isolation of any such effects. More detailed study is needed to determine the nature of the effects of a non-uniform field on a high pressure (1.0 Torr) positive column.

The discharge was created in a glass tube of radius $R=7.2$ cm. by high voltage breakdown using a cold cathode. Typical operating conditions were $V=1.5$ kV, $I=15$ mA, and $P=1.0$ Torr. Double probes were placed at two positions in the positive column, 10 and 22 cm. from the anode. The latter position was the geometric center of the hole through the magnet. In these positions, measurements were taken collecting current from both parallel and perpendicular directions with respect to the direction of the magnetic field. The two cases were equivalent according to the measurements of electron temperature and density.

Double probe measurements supported the theory of the positive column ($B=0$) in that (1) a constant electron temperature profile (vs. radius) was observed, (2) the electron temperature matched within ten percent that predicted by (Bickerton and von Engel (1932) and (3) the densities near the axis of the tube matched the Bessel function $J_0(2.405 r/R)$ from Schottky (1924). The effect of a drifting plasma (due to the electric field) did not change the temperature and density measurements for probes in any orientation in the column.

When the magnetic field was applied, the probe measurements indicated the following effects. First, it was observed that when one probe was placed behind another (behind with respect to the direction of the magnetic field), a wake effect altered the results, especially the electron temperature. Second, although the electron temperature was observed to decrease with increasing B as the theory

of Bickerton and von Engel (1950) predicts, the decrease was more rapid and the slope of the curve vanished near the 100 gauss level. Third, the increase in plasma density on the axis was somewhat more rapid than the theory of Bickerton and von Engel indicated.

Finally, the saturation ion currents agreed with the theory of Sugawara and Hatta (1965A) only when the effect of increased density was excluded from the ratio. In other words, the ratio $I_{\perp+}/I_{\parallel+}$ agreed in that it decreased as B increased. This is not surprising in that the theory neglects the size of the ion sheath with respect to the probe radius, and is derived for plane probes. Both of these conditions were not realized in the experiment. This comparison was made because the theory is the only direct attempt to determine the validity of the double probe method available in the literature.

At the present time it is not clear what effect a non-uniform field has on the double probe method. This is true in part because the theory of probes in magnetic fields is not developed to the desired degree. Experimentally this is true because one must have a known standard to measure the effect, and the behavior of a plasma in a non-uniform field in a discharge tube for example is not fully understood.

Further theoretical development of the case studied by Sugawara and Hatta should include cylindrical probes. The ion saturation currents could then be of use in determining the effect of the field on the double probe method, without the problem of wakes which are nearly unavoidable with plane double probes.

BIBLIOGRAPHY

- Allen, J.E., R.L.F. Boyd and P. Renolds, Proc. Phys. Soc. (London) B70, 297 (1957).
- Bernstein, I. and I. Rabinowitz, "Theory of Electrostatic Probes in a Low-Density Plasma", Phys. Fluids 2, 112 (1959).
- Bertotti, B., "Theory of an Electrostatic Probe in a Strong Magnetic Field I", Phys. Fluids 4, 1047 (1961).
- Bertotti, B., "Theory of an Electrostatic Probe in a Strong Magnetic Field II", Phys. Fluids 5, 1010 (1962).
- Bickerton, R.J., and A. von Engel, "The Positive Column in a Longitudinal Magnetic Field", Proc. Phys. Soc. 69, 4B 473 (1956).
- Bienkowski, G., Phys. Fluids 10, 675 (1967).
- Bohm, D., in The Characteristics of Electrical Discharges in Magnetic Fields, eds. A. Guthrie and R.K. Wakerling, McGraw-Hill, N.Y. (1949).
- Boyd, R.F., Proc. Phys. Soc. (London) B64, 795 (1951).
- Brown, S.C., Basic Data of Plasma Physics, MIT Press Cambridge, Mass. (1959).
- Brown, S.C., Introduction to Electrical Discharges in Gases, John Wiley and Sons Inc. N.Y. (1966).
- Chen, F.F., in Plasma Diagnostic Techniques, by R.H. Huddleston and S.L. Leonard, Academic Press, N.Y. (1965) Chap. 4 REFERENCE A.
- Chen, F.F., Nucl. Energy., pt. c. 7, 47 (1965) REFERENCE B.
- Chou, Y.S., R. Talbot, and D.R. Willis, "Kinetic Theory of a Spherical Electrostatic Probe in a Stationary Plasma", Phys. Fluids 9, 2150 (1966).
- Cohen, I., Phys. Fluids 6, 1492 (1963).
- Davydov, B. and L. Zmangvskaja, Tech. Phys. USSR 3, 715 (1936).
- Ecker, G., K.S. Masterson and J.J. McClure, Univ. Calif. Rad. Lab. Rept. No. UCRL-10128, TID-4500 17th ed. (1962).

- Holt, E.H., and R.E. Haskell, Foundations in Plasma Dynamics, Macmillan Co. N.Y. (1965) p. 190.
- Johnson, E.O., and L. Malter, "A Floating Double Probe Method for Measurements in Gas Discharges", Phys. Rev. 80, 1 (1950).
- Knechtli, R.C., and J.Y. Wada, Phys. Rev. Letters 6, 215 (1961).
- Lam, S.H., Phys. Fluids 8, 73, 1002 (1965).
- Langmuir, I., and H. Mott-Smith, "The Theory of Collectors in Gaseous Discharges", Phys. Rev. 28, 727 (1926).
- Langmuir, I., and K.T. Compton, Rev. Mod. Phys. 3, 91 (1931).
- Langmuir, I., and The Collected Works of I. Langmuir, ed. C.G. Suits, Pergamon Press, N.Y. (1961) vols. 3-5.
- Little, R.G., and J.F. Waymouth, "Experimentally Determined Plasma Perturbation by a Probe", Phys. Fluids 9, 801 (1966).
- Loeb, L.B., Fundamental Processes of Electrical Discharge in Gases, John Wiley and Sons Inc., N.Y. (1939).
- Sanmartin, J.R., "Theory of a Probe in a Strong Magnetic Field", Plasma Physics Lab. Matt-599 (July, 1968), Princeton Plasma Physics Lab., Princeton, N.J.
- Schottky, W., Physik Z. 25, 342, 635 (1924) and Schottky and Issendorf, Z. Physik 31, 163 (1925).
- Schulz, C.J., and S.C. Brown, Phys. Rev. 98, 1643 (1955).
- Spivak, G., and E. Reichrudel, Physik Z. Sowjetunion 9, 655 (1936); Izv. Akad. Nauk. USSR 479 (1938); and zh. Eksperim. i. Teor. Fiz. 8, 319 (1938).
- Su, C.H., and S.H. Lan, Phys. Fluids, 6, 1479 (1963).
- Su, C.H., Plasma Phys. Lab. Matt-563 (1968), Princeton Plasma Phys. Lab., Princeton, N.J.
- Sugawara, M. and Y. Hatta, J. Appl. Phys. 36, 314 (1965). REFERENCE A.
- Sugawara, M., and Y. Hatta, "Validity of the Floating Double Probe Method in a Magnetic Field", J. Appl. Phys. 36, 2361 (1965). REFERENCE B.
- Tonks, L., and I. Langmuir, Phys. Rev. 34, 867 (1929).

von Engel, A., and M. Steenbeck, Electrische Gasentladungen 1, 89, 184 and 192, Julius Springer, Berlin (1932) and cited in L.B. Loeb, 1939.

von Engel, A., Ionized Gases, Clarendon Press, Oxford (1965).

APPENDIX

As an example of the DPM, the following sample calculation of the electron temperature and plasma density is given. The data was taken by probe set number 1 in nitrogen 1 Torr, located at (0, 1, -12).

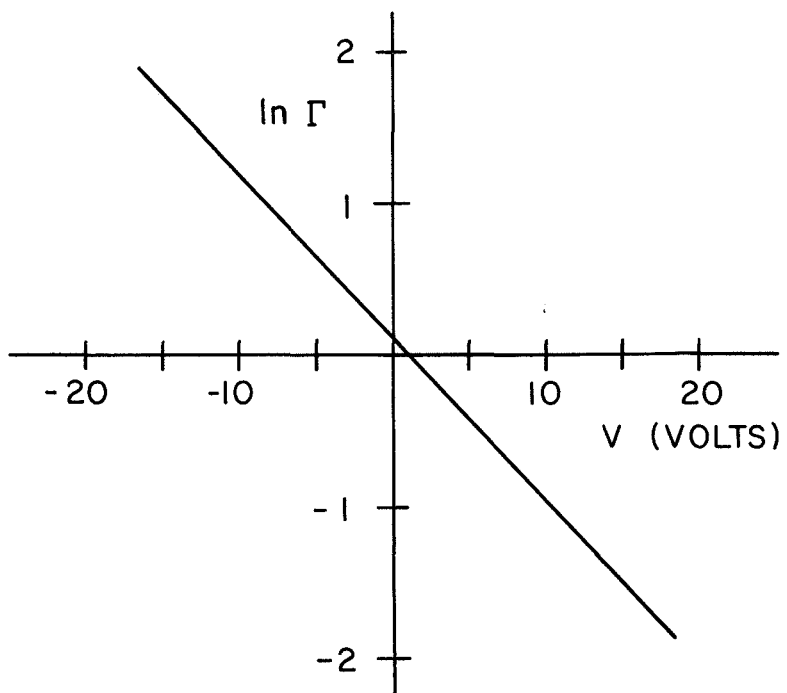
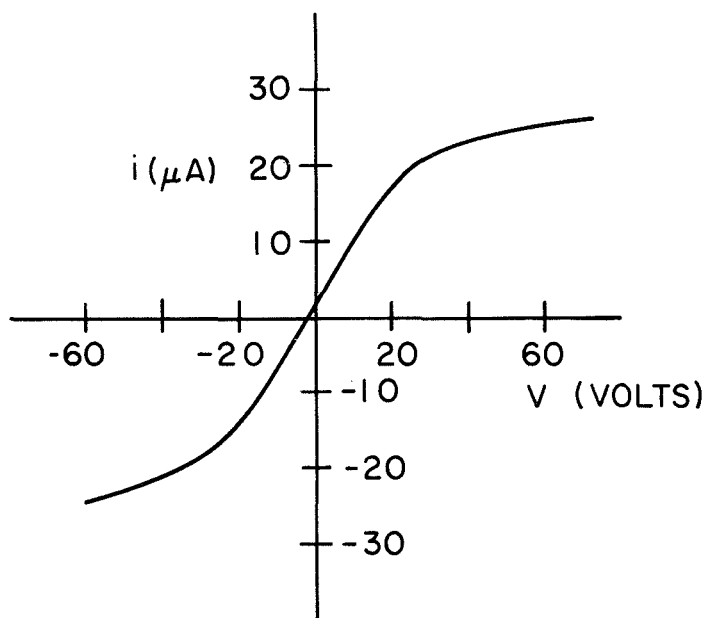
V_D	i		i_{2-}		Γ		$\ln\Gamma$	
	+V	-V	+v	-V	+	-	+	-
0	.8	.7	19.0	19.0	1.10	1.10	.09	.09
5	6.4	2.8	25.5	16.0	.65	1.62	-.43	.47
10	11.5	8.5	30.5	10.5	.37	3.0	-.99	1.09
15	14.2	11.5	33.5	7.5	.25	4.6	-1.38	1.52
20	18.1	15.2	37.0	4.0	.11	9.6	-2.20	2.26
25	20.1	17.1						
30	21.9	18.9						
35	23.2	20.2						
40	24.9	21.8						
45	25.9	22.8						
50	26.8	23.5						
55	27.2	24.2						
60	28.2	24.9						
65	28.8							

Slope ($\ln\Gamma$ vs. V_D Curve) = .1/volt.

$$T_e = \frac{1.16 \times 10^4}{.1} = 1.16 \times 10^5 \text{°k}$$

Figure 16 is the i vs. V_D curve and the $\ln\Gamma$ vs. V_D plot.

Using the following constants, we proceed to calculate the density.



SAMPLE CALCULATION CURVES

FIGURE 16

$$T_+ = 3.5 \times 10^2 \text{ } ^\circ\text{K}$$

$$m_+ = 4.65 \times 10^{-26} \text{ kg (N}_2\text{)}$$

$$m_- = 9.109 \times 10^{-31} \text{ kg}$$

$$e = 1.6 \times 10^{-19} \text{ coul.}$$

$$k = 1.38 \times 10^{-23} \text{ J/}^\circ\text{K}$$

$$\begin{aligned} \therefore V_F &= -4.31 \times 10^{-5} (1.16 \times 10^5) \ln (1.46 \times 10^2 \times 1.16 \times 10^5) \\ &= -5(16.12 + .52) = 83.2 \end{aligned}$$

$$F = 19/42 = .45$$

$$\therefore \Delta V = -8.62 \times 10^{-5} (1.16 \times 10^5) \ln F = 7.98 \times 8.0$$

$$\therefore |V| = 75.2$$

$$\beta^2 = \frac{1.465 \times 10^{-6} V^{3/2}}{i_+} = 45.5 \quad \text{use } i_{+AVE} = 21$$

From the β^2 vs. r_o/r curve labeled $(-\beta^2) \times 10^{-2}$ (Loeb, 1939, p.323).

$$r_o/r = \alpha = 12$$

$$\therefore n = \frac{4.87 \times 10^{16} i_{+AVE}}{\alpha A a} = 5.1 \times 10^{16} / \text{m}^3 = 5.1 \times 10^{10} / \text{cm}^3.$$